



This is a repository copy of *Performance and calibration of quark/gluon-jet taggers using 140 fb⁻¹ of pp collisions at $\sqrt{s} = 13$ TeV with the ATLAS detector.*

White Rose Research Online URL for this paper:

<https://eprints.whiterose.ac.uk/208708/>

Version: Published Version

Article:

Aad, G., Abbott, B., Abeling, K. et al. (2940 more authors) (2024) Performance and calibration of quark/gluon-jet taggers using 140 fb⁻¹ of pp collisions at $\sqrt{s} = 13$ TeV with the ATLAS detector. Chinese Physics C, 48 (2). 023001. ISSN 1674-1137

<https://doi.org/10.1088/1674-1137/acf701>

Reuse

This article is distributed under the terms of the Creative Commons Attribution (CC BY) licence. This licence allows you to distribute, remix, tweak, and build upon the work, even commercially, as long as you credit the authors for the original work. More information and the full terms of the licence here:

<https://creativecommons.org/licenses/>

Takedown

If you consider content in White Rose Research Online to be in breach of UK law, please notify us by emailing eprints@whiterose.ac.uk including the URL of the record and the reason for the withdrawal request.



eprints@whiterose.ac.uk
<https://eprints.whiterose.ac.uk/>

PAPER • OPEN ACCESS

Performance and calibration of quark/gluon-jet taggers using 140 fb^{-1} of pp collisions at $\sqrt{s} = 13 \text{ TeV}$ with the ATLAS detector^{*}

To cite this article: G. Aad *et al* 2024 *Chinese Phys. C* **48** 023001

View the [article online](#) for updates and enhancements.

You may also like

- [A new calibration method for charm jet identification validated with proton-proton collision events at \$s = 13 \text{ TeV}\$](#)
The CMS collaboration, Armen Tumasyan, Wolfgang Adam et al.
- [Fast \$b\$ -tagging at the high-level trigger of the ATLAS experiment in LHC Run 3](#)
G. Aad, B. Abbott, K. Abeling et al.
- [The ATLAS Fast Tracker system](#)
The ATLAS collaboration, G. Aad, B. Abbott et al.

Performance and calibration of quark/gluon-jet taggers using 140 fb^{-1} of pp collisions at $\sqrt{s} = 13 \text{ TeV}$ with the ATLAS detector*

The ATLAS Collaboration [†]

Abstract: The identification of jets originating from quarks and gluons, often referred to as quark/gluon tagging, plays an important role in various analyses performed at the Large Hadron Collider, as Standard Model measurements and searches for new particles decaying to quarks often rely on suppressing a large gluon-induced background. This paper describes the measurement of the efficiencies of quark/gluon taggers developed within the ATLAS Collaboration, using $\sqrt{s} = 13 \text{ TeV}$ proton–proton collision data with an integrated luminosity of 140 fb^{-1} collected by the ATLAS experiment. Two taggers with high performances in rejecting jets from gluon over jets from quarks are studied: one tagger is based on requirements on the number of inner-detector tracks associated with the jet, and the other combines several jet substructure observables using a boosted decision tree. A method is established to determine the quark/gluon fraction in data, by using quark/gluon-enriched subsamples defined by the jet pseudorapidity. Differences in tagging efficiency between data and simulation are provided for jets with transverse momentum between 500 GeV and 2 TeV and for multiple tagger working points.

Keywords: ATLAS, JET, QUARK, GLUON, TAGGING

DOI: 10.1088/1674-1137/acf701

I. INTRODUCTION

Various Standard Model (SM) measurements [1, 2] and searches for physics beyond the SM [3] at the Large Hadron Collider (LHC) [4] benefit from the identification of showers of hadronic particles (jets) originating from quarks or gluons. Several searches employing quark/gluon (q/g) tagging, techniques that tag jets originating from a quark or a gluon, have demonstrated improved sensitivity to new physics and the ability to discriminate between new resonances that decay into different types of hadronic jets [5–8]. For example, in some supersymmetry scenarios, many final-state light quarks can be produced [9, 10]. The ability to discriminate between

quark- and gluon-initiated jets, hereafter referred to as ‘quark-jets’ and ‘gluon-jets’, therefore provides a powerful tool to use in searches for new physics. If a new particle were discovered, such a discriminant could provide valuable information about the nature of the particle. Moreover, accurate identification of the origin of jets is crucial in certain SM measurements, such as when reconstructing hadronic decays of W bosons in a measurement of the mass of the top quark.

In the theory of quantum chromodynamics (QCD), quarks and gluons are not free particles in their kinematic evolution, and they produce streams of particles that the LHC experiments can measure. Discrimination between jets of different partonic origins has been at-

Received 1 August 2023; Accepted 7 September 2023; Published online 8 September 2023

* We acknowledge the support of ANPCyT, Argentina; YerPhI, Armenia; ARC, Australia; BMWFW and FWF, Austria; ANAS, Azerbaijan; CNPq and FAPESP, Brazil; NSERC, NRC and CFI, Canada; CERN; ANID, Chile; CAS, MOST and NSFC, China; Minciencias, Colombia; MEYS CR, Czech Republic; DNRF and DNS-RC, Denmark; IN2P3-CNRS and CEA-DRF/IRFU, France; SRNSFG, Georgia; BMBF, HGF and MPG, Germany; GSRI, Greece; RGC and Hong Kong SAR, China; ISF and Benoziyo Center, Israel; INFN, Italy; MEXT and JSPS, Japan; CNRST, Morocco; NWO, Netherlands; RCN, Norway; MEiN, Poland; FCT, Portugal; MNE/IFA, Romania; MESTD, Serbia; MSSR, Slovakia; ARRS and MIZŠ, Slovenia; DSI/NRF, South Africa; MICINN, Spain; SRC and Wallenberg Foundation, Sweden; SERI, SNSF and Cantons of Bern and Geneva, Switzerland; MOST, Taipei; TENMAK, Türkiye; STFC, United Kingdom; DOE and NSF, United States of America. In addition, individual groups and members have received support from BCKDF, CANARIE, CRC and DRAC, Canada; PRIMUS 21/SCI/017 and UNCE SCI/013, Czech Republic; COST, ERC, ERDF, Horizon 2020, ICSC-Next Generation EU and Marie Skłodowska-Curie Actions, European Union; Investissements d’Avenir Labex, Investissements d’Avenir IDEX and ANR, France; DFG and AvH Foundation, Germany; Herakleitos, Thales and Aristeia programmes co-financed by EU-ESF and the Greek NSRF, Greece; BSF-NSF and MINERVA, Israel; Norwegian Financial Mechanism 2014-2021, Norway; NCN and NAWA, Poland; La Caixa Banking Foundation, CERCA Programme Generalitat de Catalunya and PROMETEO and GenT Programmes Generalitat Valenciana, Spain; Göran Gustafssons Stiftelse, Sweden; The Royal Society and Leverhulme Trust, United Kingdom.

[†] E-mail: atlas.publications@cern.ch



Content from this work may be used under the terms of the Creative Commons Attribution 3.0 licence. Any further distribution of this work must maintain attribution to the author(s) and the title of the work, journal citation and DOI. Article funded by SCOAP³ and published under licence by Chinese Physical Society and the Institute of High Energy Physics of the Chinese Academy of Sciences and the Institute of Modern Physics of the Chinese Academy of Sciences and IOP Publishing Ltd

tempted at several experiments [11–25]. For example, some analyses [26, 27] used the full radiation pattern inside a jet as an image processed in a deep neural network classifier. Most work has relied on jet properties that result from the different colour charges of the partons. According to QCD, the colour charge of a gluon is larger than that of a quark by a factor of $9/4$ (the ‘Casimir ratio’) [28]. Hence, in their kinematic evolution and hadronisation, the gluons produce more particles, leading to jets with a higher number of constituents and a broader radiation pattern than in quark-jets. Advances in the theoretical [29] and phenomenological [30–33] understanding of the radiation patterns of quark- and gluon-jets have led to recent progress in q/g tagging. Compared to previous studies which considered single-variable taggers for a lower p_T range [34, 35], this study focuses on the construction of a new q/g tagger that utilises several jet substructure variables, and on extending the q/g tagging of jets to a higher energy range.

This paper investigates the performance of two q/g taggers, which are built with the goal of identifying quark-jets and rejecting gluon-jets. The first tagger is based on a requirement placed on the charged-particle multiplicity (n_{track}) of a jet. The second tagger employs a boosted decision tree (BDT) that takes as input a set of jet kinematic and substructure variables. The q/g tagging efficiencies are estimated in data by using a method that splits the data sample into subsamples where the fraction of quark-jets is higher or lower than the fraction of gluon-jets (i.e. quark- or gluon-enriched subsamples, respectively).

The paper is structured as follows. Section II introduces the ATLAS detector. A brief description of the data and Monte Carlo (MC) samples used in the analysis is given in Section III. In Section IV the object definitions and event selection criteria used to select events and classify them into the various categories are described. Variables used in the definition of the q/g taggers studied in this analysis are presented in Section V. The method developed to evaluate the q/g tagging efficiencies and the taggers’ discrimination power is presented in Section VI. Systematic uncertainties affecting the analysis are detailed in Section VII. Measurements of the tagging efficiencies in data and their ratio to those expected from MC simulation (scale factors) are shown in Section VIII, while conclusions are drawn in Section IX.

II. ATLAS DETECTOR

The ATLAS detector [36] at the LHC covers nearly the entire solid angle around the collision point.¹⁾ It con-

sists of an inner tracking detector surrounded by a thin superconducting solenoid, electromagnetic and hadron calorimeters, and a muon spectrometer incorporating three large superconducting air-core toroidal magnets.

The inner-detector system (ID) is immersed in a 2 T axial magnetic field and provides charged-particle tracking in the range $|\eta| < 2.5$. The high-granularity silicon pixel detector covers the vertex region and typically provides four measurements per track, the first hit normally being in the insertable B-layer, which was installed before Run 2 [37]. It is followed by the silicon microstrip tracker, which usually provides eight measurements per track. These silicon detectors are complemented by the transition radiation tracker (TRT), which enables radially extended track reconstruction up to $|\eta| = 2.0$. The TRT also provides electron identification information based on the fraction of hits (typically 30 in total) above a higher energy-deposit threshold corresponding to transition radiation.

The calorimeter system covers the range $|\eta| < 4.9$. Within the region $|\eta| < 3.2$, electromagnetic calorimetry is provided by barrel and endcap high-granularity lead/liquid-argon (LAr) calorimeters, with an additional thin LAr presampler covering $|\eta| < 1.8$ to correct for energy loss in material upstream of the calorimeters. Hadron calorimetry is provided by the steel/scintillator-tile calorimeter, segmented into three barrel structures within $|\eta| < 1.7$, and two copper/LAr hadron endcap calorimeters. The solid angle coverage is completed with forward copper/LAr and tungsten/LAr calorimeter modules optimised for electromagnetic and hadronic energy measurements, respectively.

The muon spectrometer comprises separate trigger and high-precision tracking chambers measuring the deflection of muons in a magnetic field generated by the superconducting air-core toroidal magnets. The field integral of the toroids ranges between 2.0 and 6.0 T m across most of the detector. Three layers of precision chambers, each consisting of layers of monitored drift tubes, cover the region $|\eta| < 2.7$. They are complemented by cathodestrip chambers in the forward region, where the background is highest. The muon trigger system covers the range $|\eta| < 2.4$ with resistive-plate chambers in the barrel and thin-gap chambers in the endcap regions.

Interesting events are selected by the first-level trigger system implemented in custom hardware, followed by selections made by algorithms implemented in software in the high-level trigger [38]. The first-level trigger accepts events from the 40 MHz bunch crossings at a rate below 100 kHz, which the high-level trigger reduces in

¹⁾ ATLAS uses a right-handed coordinate system with its origin at the nominal interaction point (IP) in the centre of the detector and the z -axis along the beam pipe. The x -axis points from the IP to the centre of the LHC ring, and the y -axis points upwards. Cylindrical coordinates (r, ϕ) are used in the transverse plane, ϕ being the azimuthal angle around the z -axis. The pseudorapidity is defined in terms of the polar angle θ as $\eta = -\ln \tan(\theta/2)$. Angular distance is measured in units of $\Delta R \equiv \sqrt{(\Delta\eta)^2 + (\Delta\phi)^2}$.

order to record events to disk at about 1 kHz.

An extensive software suite [39] is used in data simulation, the reconstruction and analysis of real and simulated data, in detector operations, and in the trigger and data acquisition systems of the experiment.

III. DATA AND SIMULATION SAMPLES

The data used in this analysis were collected by the ATLAS detector between 2015 and 2018 from proton–proton collisions at a centre-of-mass energy of $\sqrt{s} = 13$ TeV, and correspond to an integrated luminosity of 140 fb⁻¹ [40]. The events included in this dataset satisfy quality requirements which ensure that all detector systems were operational [41]. This was achieved by monitoring detector-level quantities and the characteristics of reconstructed collision events at key stages of the data processing chain.

MC simulations are used to model SM multijet production, which is the main process expected to play a role in this analysis. The Pythia 8.230 [42] generator was used to simulate multijet production with a QCD matrix element (ME) calculation and leading-order (LO) accuracy in the parton shower evolution. The NNPDF2.3lo parton distribution function (PDF) [43] set was used, and Pythia internal parameter values were set according to the A14 tune [44]. The Pythia 8.230 MC sample is taken as the default choice to obtain the nominal result, as it has been tested extensively in previous ATLAS analyses [45, 46] and has been seen to accurately describe the data [47].

Several alternative MC samples are used for the estimation of uncertainties coming from hadronisation modelling. Two sets of MC samples were produced using the Sherpa 2.2.5 [48] generator, with the same ME for the $2 \rightarrow 2$ process at LO, the same parton shower configurations based on Catani–Seymour dipole factorisation [49], and the same CT14nnlo PDF set [50], but different hadronisation algorithms. The first set of samples uses the dedicated Sherpa AHADIC model for hadronisation [51], based on cluster fragmentation. The second set of samples was generated with the same configuration but using the Sherpa interface to the Lund string fragmentation model of Pythia 6 [52] and its decay tables.

Two multijet MC samples were generated at next-to-leading order (NLO) by Herwig 7.1.3 [53] with the same MMHT2014nlo [54] PDF set and hadronisation model, but with one using of the default parton shower model with angular ordering and the other using the dipole shower as an alternative, allowing an estimation of the effect of the shower model on the results.

Another set of QCD multijet samples with NLO precision in the ME is also included for the ME uncertainty estimation. They were generated with Powheg Box v2 [55–57] and interfaced to Pythia for the parton shower and hadronisation models. The NNPDF3.0nlo [58] PDF

set was used for these samples.

IV. OBJECT RECONSTRUCTION AND EVENT SELECTION

Jets are reconstructed with the anti- k_r algorithm [59] with a radius parameter of $R = 0.4$ using as constituents particle-flow (PFlow) objects [60], with the combined information from the ID and the calorimeter. Reconstructed jets are considered isolated if there is no other reconstructed jet within a cone of size $\Delta R = 0.7$ around the jet axis. Only isolated jets are considered in this study. An overall jet energy calibration [61] is performed with a sequence of simulation-based corrections and in situ calibrations, which accounts for residual detector effects as well as contributions from the effects of multiple simultaneous pp collisions (pile-up). Only light-flavoured quark-jets (u, d, s) are considered in this study.

Tracks arising from charged particles are reconstructed [62] from the hits in the ID and are required to have transverse momentum $p_T > 500$ MeV, $|\eta| < 2.5$, at least one pixel hit and at least six hits in the silicon microstrip tracker, as well as transverse and longitudinal impact parameters with respect to the hard-scattering vertex that satisfy $|d_0| < 1$ mm and $|z_0 \sin(\theta)| < 1$ mm respectively. Additionally, the event is required to have at least one vertex with two or more associated tracks. The vertex with the highest p_T^2 sum of the associated tracks is considered to be the primary vertex. The ghost-association technique [63] is employed to match tracks to jets; tracks are treated as four-vectors of infinitesimal magnitude during the jet reconstruction and are then assigned to the jet with which they are clustered.

A second jet collection used is called ‘truth jets’ [61]. Truth jets are reconstructed from stable final-state particles from the simulation samples, using the same anti- k_r $R = 0.4$ algorithm as PFlow jets. They are geometrically matched to PFlow jets by requiring that their angular separation satisfies $\Delta R < 0.4$. Truth jets are assigned a flavour label [34, 35], called ‘truth label’. The truth label of a jet is defined by the flavour of the highest-energy parton in the parton shower, before hadronisation, within a cone of size $\Delta R = 0.4$ around the jet axis. Using this definition, jets that originate from gluons splitting into b -quark or c -quark pairs are labelled as heavy-flavour jets, which are often identified by the presence of long-lived or leptonically decaying hadrons, and thus no special discriminant for heavy-flavour quarks is used here [64, 65]. Jets remain unlabelled if no truth parton with $p_T > 1$ GeV is found within the cone surrounding the truth jet. Unlabelled jets typically arise from pile-up, and are less than 1% of the dataset at $p_T > 500$ GeV. They are thus ignored [66].

Events used in the analysis were selected with a single-jet trigger, and must have at least two jets with

$p_T > 500$ GeV. The two leading jets must each have $|\eta| < 2.1$ to guarantee that they are well within the acceptance of the tracking detector. The ratio of the leading jet's p_T to the sub-leading jet's p_T is required to be less than 1.5, to select a sample in which the two jets are balanced in p_T . The two leading- p_T jets are used to define quark-enriched and gluon-enriched subsamples.

For each selected jet pair, the jet with the higher $|\eta|$ value is selected to populate the quark-enriched sample. The other jet, which has a lower $|\eta|$ value, is assigned to a gluon-enriched sample. This selection strategy leverages the fact that in the high proton-momentum-fraction range, the PDF has a higher probability of including valence-quarks. Consequently, the ensemble of jets which are more forward (higher $|\eta|$) have a higher probability of being quark-jets, whereas the ensemble of jets which are more central (lower $|\eta|$) have a higher probability of being gluon-jets [67]. This is illustrated later for the Pythia MC multijet sample, in Figure 2, where the quark-jet fraction is higher in the forward region than in the central region and also increases with jet p_T .

V. TAGGER DEFINITIONS

Jet substructure variables are useful in developing q/g taggers, given the predicted difference between the radiation patterns of quark- and gluon-jets. A variable well suited to this task is the track multiplicity, as gluon-jets are expected to have more constituents than quark-jets. Hence, the n_{track} in a jet can be used to define a single-variable q/g tagger by imposing a requirement on its value. In this analysis, a more advanced q/g tagger based on a BDT is also developed, using information about the jet p_T , n_{track} , the jet track width w^{track} [34, 68], and the two-point energy correlation function $C_1^{\beta=0.2}$ [69, 70], which takes into account the energy distribution within the jet.¹⁾ The $|\eta|$ of a jet is not used as an input to the BDT, as it could interfere with the definition of the quark- and gluon-enriched samples and distort the estimation of the fractions of quark- and gluon-jets using the method presented in Section VI.

The BDT-tagger is trained using 60 million events with two jets from Pythia MC samples described in Section III, with a dataset distribution of 8:1:1 for training, validation, and testing, respectively. For the simulated events employed in the BDT training process, an additional processing step is implemented to obtain a flattened distribution of the p_T spectra for quark- and gluon-jets. This step aims to emphasise the training for

jets in the tail of the p_T spectrum, and to equalise the numbers of quark- and gluon-jets in the training. In training procedure, the LGBMClassifier from the lightGBM [71] framework is used, with Optuna [72] for hyperparameter tuning. A score is assigned to each BDT that goes into the boosting process based on its error rate. After 100 iterations of this procedure, a stable BDT is established, defined with 224 leaves. The BDT score is used to classify a jet as a quark-jet or a gluon-jet.

The performance of a jet tagger is evaluated using a receiver operating characteristic (ROC) curve defined from the quark- and gluon-jet efficiencies. The area under the ROC curve (AUC) is used as a metric to quantify the effectiveness of a tagger, with a larger AUC value indicating better performance. Figure 1 shows the performance of jet tagging variables. The BDT performs better than individual jet-substructure variables, meaning that the BDT-tagger can reject more gluon-jets than the n_{track} -only tagger at the same quark-jet efficiency. Since the tagging variables strongly depend on the p_T of a jet, performances and comparisons among taggers are given in different jet- p_T bins with boundaries at 500, 600, 800, 1000, 1200, 1500 and 2000 GeV.

VI. MATRIX METHOD

Evaluating the performance of the q/g taggers under study needs samples containing solely quark- or gluon-jets. To extract the q/g tagging-variable distribution shapes for quark- and gluon-jets in the data, a method that exploits samples with different q/g fractions is used, called the matrix method [35].

In the matrix method, the distribution of a jet variable x for forward jets, $p_F(x)$, and for central jets, $p_C(x)$, can be written as:

$$\begin{pmatrix} p_F(x) \\ p_C(x) \end{pmatrix} = \underbrace{\begin{pmatrix} f_{F,Q} & f_{F,G} \\ f_{C,Q} & f_{C,G} \end{pmatrix}}_{\equiv F} \begin{pmatrix} p_Q(x) \\ p_G(x) \end{pmatrix}. \quad (1)$$

Here $p_Q(x)$ and $p_G(x)$ are the distributions of the variable x for pure quark- and gluon-jets, respectively, and the matrix F contains the fractions of quark- or gluon-jets in the samples of jets in the forward/central region. Such fractions are taken from MC simulation and are shown in Fig. 2 for the Pythia MC samples. The matrix method allows $p_Q(x)$ and $p_G(x)$ to be extracted by inverting the matrix F for every p_T range considered.

1) The jet track width is defined as $w^{\text{track}} = \frac{\sum_{\text{track} \in \text{jet}} p_T^{\text{track}} \Delta R_{\text{track,jet}}}{\sum_{\text{track} \in \text{jet}} p_T^{\text{track}}}$, where p_T^{track} is the p_T of a charged track associated to the jet. The two-point energy correlation function instead is defined as $C_1^{\beta=0.2} = \frac{\sum_{i \neq j} p_{T,i} p_{T,j} (\Delta R_{i,j})^{\beta=0.2}}{(\sum_{\text{track} \in \text{jet}} p_T^{\text{track}})^2}$, where i and j denote tracks associated with the jet and the sum runs over all the combinations of two tracks. The parameter β is fixed to 0.2, which is known to be suitable for q/g tagging.

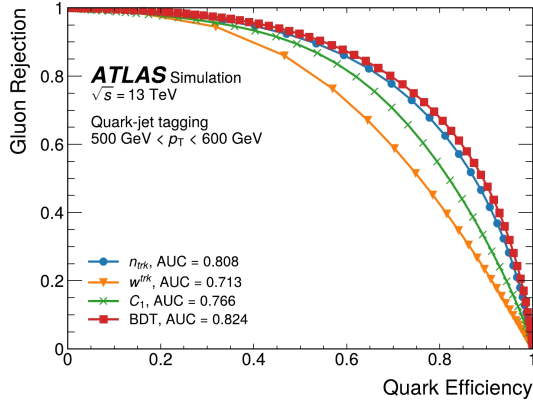


Fig. 1. (color online) ROC curves for quark-jet tagging variables, using the Pythia MC sample.

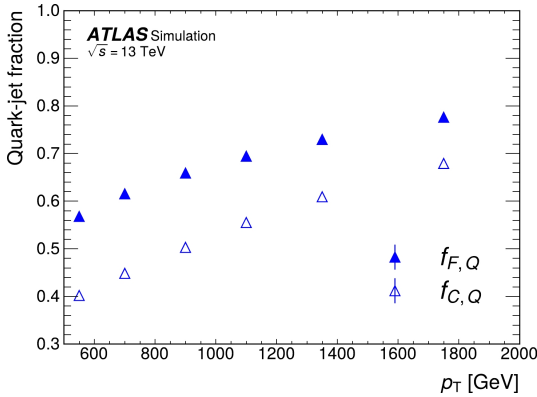


Fig. 2. (color online) Fractions of quark-jets in the forward (triangles) and the central regions (open triangles) from the Pythia MC multijet sample. The statistical uncertainty is smaller than the marker size.

Equation (1) is valid if it is assumed that the shapes of $p_Q(x)$ and $p_G(x)$ do not depend on whether the jets are in the central region or the forward region. Jet fragmentation at a *pp* collider is expected to be mainly governed by the jet p_T and is generally considered independent of η in accordance with the parton type. Therefore, an approach to extract distributions derived from the quark-jets' and gluon-jets' radiation patterns should be valid at the particle level. At the detector level, however, the measured radiation pattern inside jets is no longer independent of η , since changes in detector material and technology may cause variations in the response and introduce differences between the central and forward regions. These effects result in a non-closure of the matrix method.

A re-weighting procedure is applied to accommodate this feature and to ensure that the distributions of the jet tagging variables in the central and forward regions match. For each event, the central jet is weighted by a so-called re-weighting factor:

$$w(x) = \frac{p_F(x)}{p_C(x)}.$$

Even if the re-weighting factor corrects for an effect that is, at first order, independent on the origin of the jet, $w(x)$ can be calculated separately for truth-labelled quark-jets and gluon-jets. By default, the re-weighting factor obtained from truth-labelled quark-jets is applied to both the quark-jets and gluon-jets, while the re-weighting factor obtained from truth-labelled gluon-jets is used as an alternative to evaluate the systematic uncertainty associated with the re-weighting procedure.

After re-weighting, the extracted $p_Q(x)$ and $p_G(x)$ distributions exhibit good agreement with the truth distributions, as shown in Fig. 3. The shapes of the $p_Q(x)$ and $p_G(x)$ distributions extracted from the Pythia MC samples are similar to those in data, with differences within 25%, hence validating the method. A residual non-closure of a few percent still remains, as shown in the middle panel of Figs. 3(a)–3(d), and is taken as an MC non-closure systematic uncertainty, as described in Section VII.

The tagger working points (WP) are defined for fixed quark-jets efficiency in the nominal Pythia MC sample, for both taggers. The efficiencies for quark- and gluon-jets at a given WP are defined as:

$$\epsilon_{Q/G}(x^{\text{WP}}) = \int_{x < x^{\text{WP}}} p_{Q/G}(x) dx. \quad (2)$$

Rejection factors for quark- and gluon-jets can also be defined, as:

$$\xi_{Q/G}(x^{\text{WP}}) = 1 / \int_{x > x^{\text{WP}}} p_{Q/G}(x) dx = 1 / (1 - \epsilon_{Q/G}(x^{\text{WP}})). \quad (3)$$

Differences between the quark-jet tagging efficiencies and gluon-jet rejection measured in data and the ones extracted from MC samples are described by data-to-MC scale factors (SF), for each *q/g* tagger and in various p_T bins, at a fixed WP. The SF is defined using Eqs. (2) and (3) for quark- and gluon-jets, respectively:

$$\text{SF}_Q(x^{\text{WP}}) = \frac{\epsilon_Q^{\text{Data}}(x^{\text{WP}})}{\epsilon_Q^{\text{MC}}(x^{\text{WP}})} \quad (4)$$

$$\text{SF}_G(x^{\text{WP}}) = \frac{\xi_G^{\text{Data}}(x^{\text{WP}})}{\xi_G^{\text{MC}}(x^{\text{WP}})}, \quad (5)$$

where $\epsilon_{Q/G}^{\text{Data}}(x^{\text{WP}})$ and $\epsilon_{Q/G}^{\text{MC}}(x^{\text{WP}})$ are $\epsilon_{Q/G}(x^{\text{WP}})$ in data and MC samples, respectively. The same definitions apply to $\xi_{Q/G}(x^{\text{WP}})$. The WPs corresponding to 50%, 60%, 70% and 80% fixed quark-jets tagging efficiency have been studied and their corresponding SFs exhibit similar characteristics. The results for the 50% WP are shown in Section VIII.

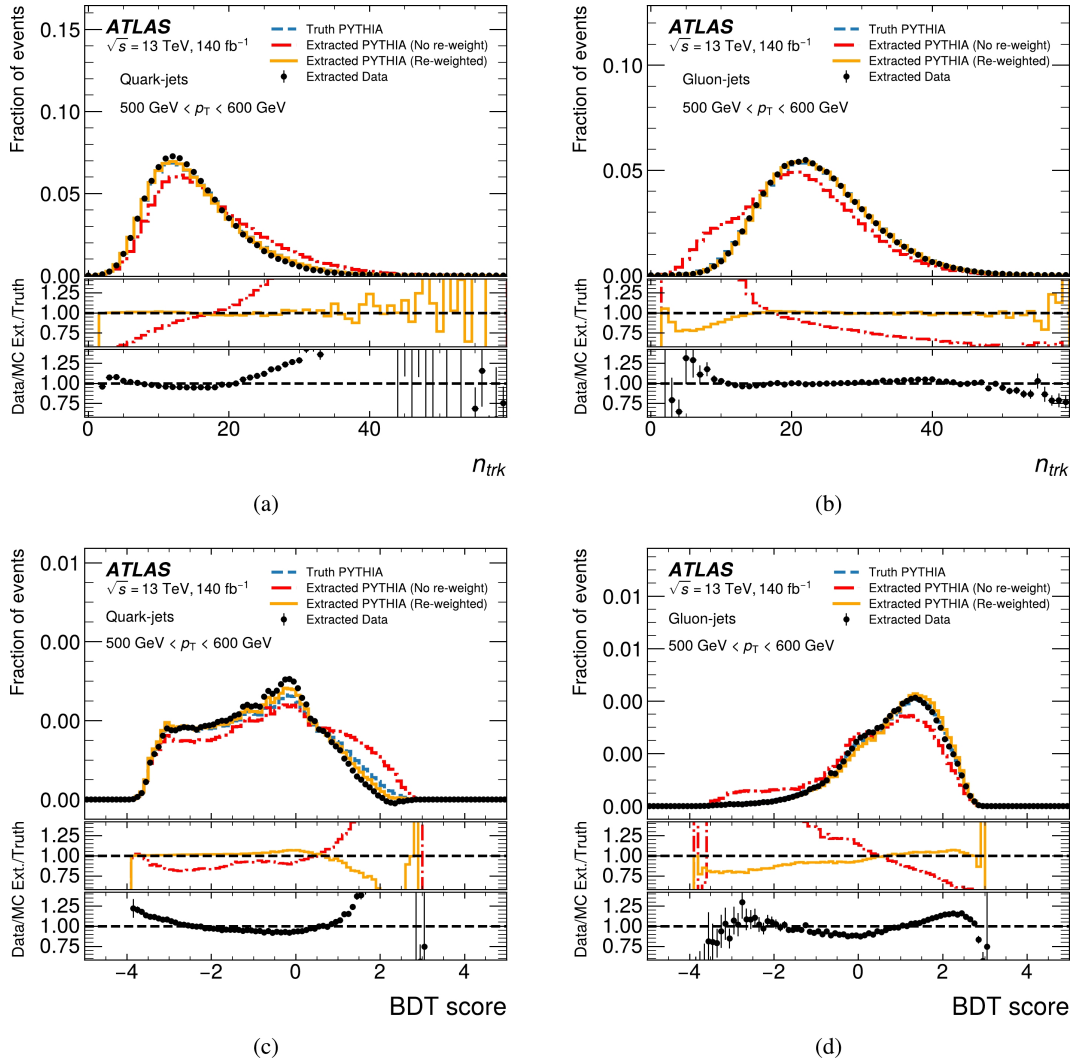


Fig. 3. (color online) The distributions of n_{track} (a,b) and BDT score (c,d) in quark-jets (left) and gluon-jets (right) in the p_T range between 500 GeV and 600 GeV obtained from truth Pythia (dashed line), extracted Pythia before re-weighting (dash dotted line) and after re-weighting (solid line), and extracted data (dots) are shown in the top panel. The middle panel shows the ratio of extracted Pythia to truth Pythia. The bottom panel shows the ratio of extracted data to extracted Pythia after re-weighting.

VII. SYSTEMATIC UNCERTAINTIES

Several sources of systematic uncertainty affect the measurement of the SFs. Theoretical uncertainties arise from the modelling in the MC simulation, due to the choice of matrix element, parton showering model, PDF, renormalisation and factorisation scales, and hadronisation model. The experimental uncertainties coming from the calibration of the jet energy scale (JES) and jet energy resolution (JER) [73] and from track reconstruction are also taken into account. Uncertainties due to methodology, such as the one associated with the re-weighting procedure and the residual MC non-closure, are also considered and propagated to the final SF measurements.

A. Theoretical uncertainty

The uncertainty due to the modelling of the parton

shower is obtained by comparing SFs in two Herwig MC samples with the same ME and hadronisation model but different shower algorithms, as described in Section III; this uncertainty varies between 1% and 9%. The systematic uncertainty due to the hadronisation modelling is estimated as the difference between the SFs obtained with two Sherpa MC samples with different hadronisation models; this uncertainty ranges between 1% and 8%. An additional uncertainty covering the calculation of the ME and its matching to the parton shower algorithm is estimated from the differences between the SFs extracted using Powheg+Pythia and Pythia MC samples. This uncertainty amounts to approximately 1% to 4%.

The uncertainty due to the chosen PDF is evaluated using the LHAPDF recommendations [74]. The uncertainty is estimated using the variations of the NNPDF2.3lo PDF set in the nominal Pythia MC sample,

and it amounts to 5%–7%.

Variations of the renormalisation (μ_r) and factorisation (μ_f) scales for initial- and final-state radiation are used as scale uncertainties to estimate the uncertainty due to missing higher-order corrections. Seven variations of (μ_r , μ_f), with their nominal values multiplied by factors of (0.5, 0.5), (0.5, 1), (1, 0.5), (1, 1), (2, 1), (1, 2) and (2, 2), are used for the uncertainty, which is estimated from the envelope of the SFs obtained from such variations in Pythia MC samples. The uncertainty amounts to approximately 4% to 7%.

The splitting-*Kernel* variations [75] pertain to modifications of the non-singular part of the splitting functions for initial-state radiation and final-state radiation, since significant uncertainties in the non-singular terms indicate more matched matrix elements included in the computation. The uncertainty is estimated by taking the envelope of the variations of non-singular terms and it is less than 1%.

In total, the whole theoretical uncertainty amounts to approximately 18% for both taggers and is found to be the main source of uncertainty.

B. Experimental uncertainty

Experimental uncertainties come from two sources: tracking efficiencies and the JES/JER calibration. The number of associated tracks is the most important input for both taggers, and the tracking-related systematic uncertainties can impact the SF measurements. The uncertainty in the number of reconstructed tracks is split into two terms: the uncertainty in the track reconstruction efficiency and the fake-track rate [62]. Both uncertainty sources are taken into account to recalculate the number of tracks associated with jets. The track reconstruction efficiency is affected by detector material uncertainties, which are the dominant source, and the physics model. They are estimated by comparing the track reconstruction efficiencies in MC samples with varied detector modelling. The fake-track rate uncertainty is estimated from a data-to-MC comparison of the evolution of the non-linear component of the track multiplicity as a function of the average mean number of interactions per bunch crossing. The tracking systematic uncertainty is obtained from changes in the SFs after applying the systematic variations and is approximately 1% to 8%.

The JES uncertainties [73] arise from calibrating the transverse momentum balance between central and forward jets, as well as accounting for single-particle and test-beam uncertainties. The JER uncertainties consider the JER difference between data and MC samples, by studying the dijet p_T balance asymmetry. An SF is obtained for each JES/JER variation, and the change from the nominal SF value is taken as the systematic uncertainty. The total JES/JER uncertainty is approximately 0.2%.

C. Methodological uncertainty

Uncertainties associated with the matrix method come from the re-weighting process and the residual MC non-closure. In estimating the systematic uncertainty from the re-weighting process, the weights obtained from truth-labelled gluon-jets are used as an alternative, as explained in Section VI. The resulting impact on the SFs is small (between 0.1% and 0.5%) across the whole p_T range considered. The residual MC non-closure, which is observed after the re-weighting procedure, affects the SFs at the 1% level for both q/g taggers studied.

The statistical uncertainty is calculated by varying the input data distributions bin-by-bin using a Poisson distribution with the number of events in each bin as the central value. The same procedure is applied to the MC samples, but using a Gaussian distribution. Each variation of the input distributions is used as an input to the matrix method. This procedure is repeated 5000 times, with the standard deviation of the uncertainties from all pseudo-datasets taken to be the statistical uncertainty of the scale factor. This uncertainty is approximately 0.1%.

VIII. RESULTS

Figure 4 shows the gluon-jets efficiency factor defined by Eq. (2) as a function of jet p_T in both the MC samples and data, for the 50% quark-jets efficiency WP (50% WP). For this WP, around 90% of the gluon-jets are rejected by the n_{track} -only tagger, while approximately 93% of gluon-jets are rejected by the BDT-tagger. The BDT-tagger is found to perform better or as well as the n_{track} -only tagger, i.e. it has a lower gluon-jet efficiency at the same WP. This is because the BDT-tagger includes more jet substructure variables. The difference between the gluon-jets efficiency in data and MC samples increases with increasing jet p_T , which is related to the MC modelling of gluons being different from the actual data.

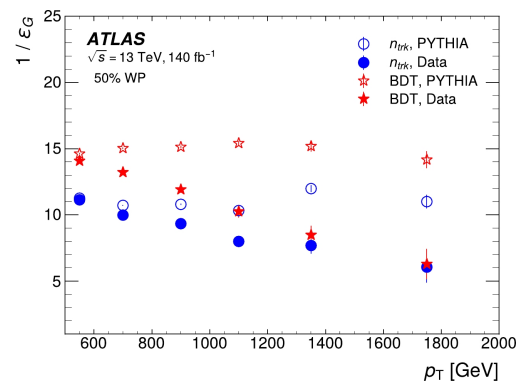


Fig. 4. (color online) Inverse of the gluon-jet efficiency for the n_{track} -only tagger (circles) and BDT-tagger (stars) as a function of jet p_T at the 50% WP in data (closed symbols) and the Pythia MC sample (open symbols). The vertical error bars show the statistical uncertainty.

Such effect is more significant for the BDT-tagger.

Figure 5 shows that the SFs for both quark-jets and gluon-jets at the 50% quark-jets efficiency WP are between 0.92 and 1.02, with a total systematic uncertainty of about 20%. The dominant source of systematic uncertainty is theoretical modelling. Tests were performed to check the stability of the results versus $|\eta|$. The SF measurements were repeated after flattening the jet $|\eta|$ of the quark-/gluon-enriched subsamples. These alternative results are compatible with the nominal ones, within the total uncertainty reported.

Since analyses interested in using the results reported in Fig. 5 may use different MC samples, a MC-to-MC SF is obtained by using each of the alternative MC samples and treating the Pythia MC samples as pseudo-data, to account for modelling differences between the Pythia and alternative MC samples. The MC-to-MC SFs for both jet taggers vary from 0.9 to 1.1 for most MC samples, as shown in Fig. 6. There are relatively large gluon modelling differences between the Herwig dipole parton shower and the Pythia parton shower, resulting in large MC-to-MC SFs.

IX. CONCLUSION

The performance of taggers for quark- and gluon-ini-

tiated jets is studied using 140 fb^{-1} of data from pp collisions at $\sqrt{s} = 13 \text{ TeV}$ collected by the ATLAS detector at the LHC, taking full advantage of the large dataset recorded from 2015 to 2018 to extend the taggers' reach to high jet energy. Two methods of jet tagging are investigated: a BDT-tagger, which combines several jet substructure observables, and a tagger based on the charged-particle jet-constituent multiplicity n_{track} . A matrix method is used to estimate the distribution shape of the tagging variables for quark- and gluon-jets, by combining information from quark-enriched and gluon-enriched samples obtained from a selection of two-jet events with jet p_T ranging from 500 GeV to 2 TeV. The variables considered are found to be described adequately by the MC, as differences with respect to ones measured in data are found to be smaller than 25%, in all the different regions defined. When tested in data, the BDT-tagger is found to have better performance than the n_{track} -only tagger in selecting quark-jets over gluon-jets between 500 GeV and 1200 GeV, while above this range, the performance of the two taggers is comparable. For a fixed quark-jet efficiency of 50%, the n_{track} -only tagger is able to reject approximately 90% of gluon-jets, while the BDT-tagger is able to reject approximately 93% of gluon-jets. A measurement of tagger performance differences in data and MC samples is provided through the definition of

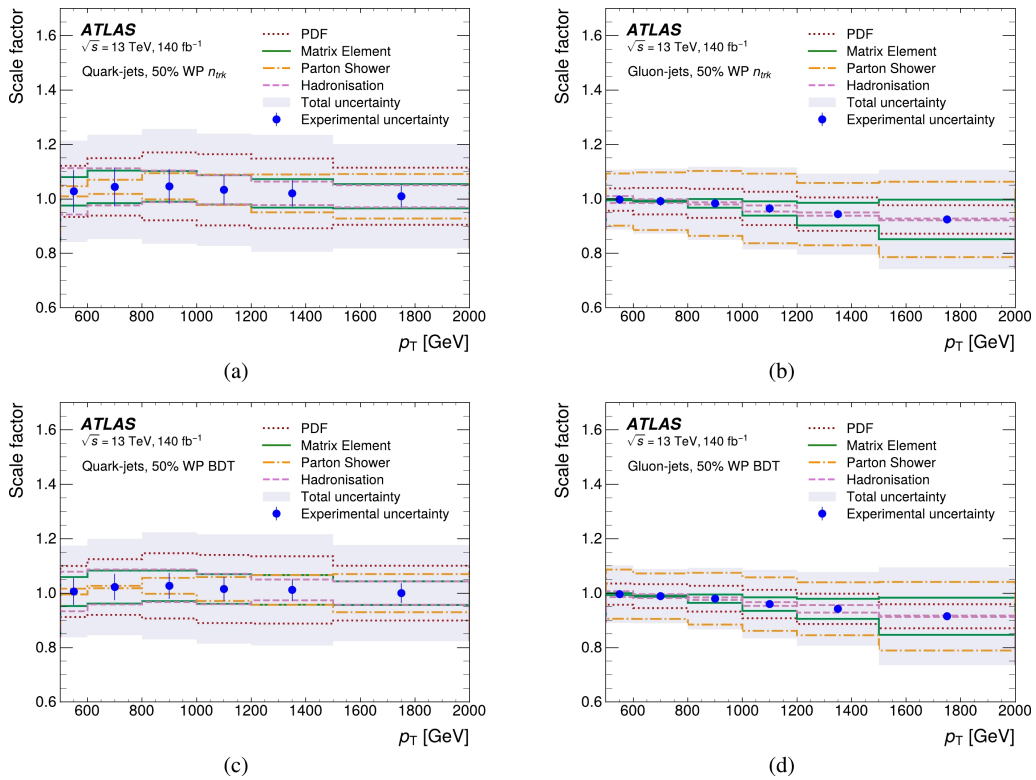


Fig. 5. (color online) The scale factors (dots) defined in Eq. (5) with the total uncertainty (band), leading theoretical uncertainties (lines) and experimental uncertainty (vertical error bar) of the n_{track} -only tagger (a,b) and the BDT-tagger (c,d) as a function of jet p_T for quark-jets (left) and gluon-jets (right) at the 50% WP using the Pythia MC sample.

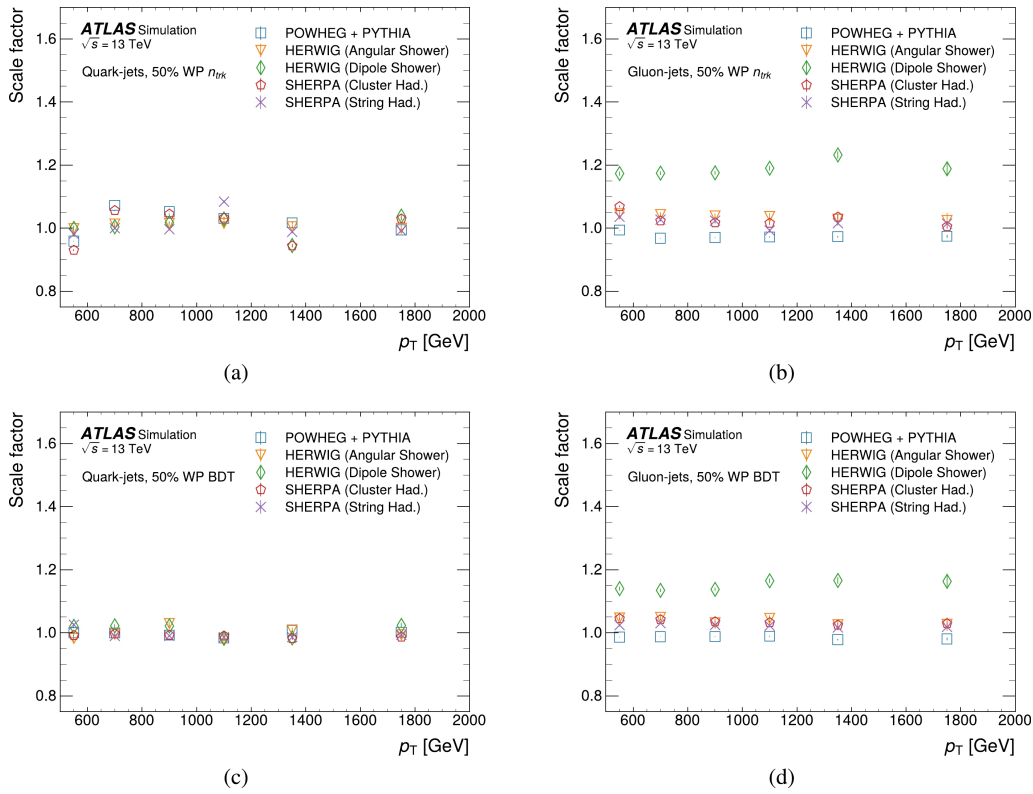


Fig. 6. (color online) The MC-to-MC scale factor for the n_{track} -only tagger (a,b) and BDT-tagger (c,d) as a function of jet p_T for quark-jets (left) and gluon-jets (right) at the 50% WP. The vertical error bars show the statistical uncertainty.

data-to-MC scale factors. The scale factors are measured in different jet- p_T intervals and are found to range from 0.92 to 1.02, with a total uncertainty of around 20% which increases at higher p_T . The main source of uncertainty comes from the different modelling choices in MC simulation and amounts to approximately 18% for both taggers. To account for differences among various MC generators, MC-to-MC scale factors are also provided, ranging from 0.9 to 1.1 for most MC samples. The q/g taggers developed in this article and the measurement of their SFs will benefit various analyses such as SM measurements that rely on the correct identification of jet origins, or new physics searches by enhancing their sensitivity to the presence of new particles.



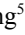
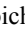

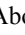


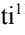
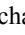


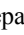







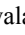




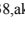
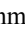

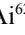
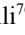

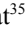
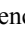
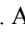




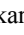
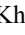
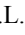



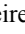

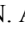











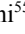
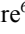
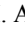
ACKNOWLEDGEMENTS

We thank CERN for the very successful operation of the LHC, as well as the support staff from our institutions without whom ATLAS could not be operated efficiently. The crucial computing support from all WLCG partners is acknowledged gratefully, in particular from CERN, the ATLAS Tier-1 facilities at TRIUMF (Canada), NDGF (Denmark, Norway, Sweden), CC-IN2P3 (France), KIT/GridKA (Germany), INFN-CNAF (Italy), NL-T1 (Netherlands), PIC (Spain), RAL (UK) and BNL (USA), the Tier-2 facilities worldwide and large non-WLCG resource providers. Major contributors of computing resources are listed in Ref. [76].

References

- [1] ATLAS Collaboration, *JHEP* **11**, 112 (2016)
- [2] CMS Collaboration, *Eur. Phys. J. C* **78**, 589 (2018)
- [3] ATLAS Collaboration, *Phys. Lett. B* **777**, 91 (2018)
- [4] L. Evans and P. Bryant, **3**, S08001 (2008)
- [5] A. K. Nayak, S. K. Rai, and T. Samui, *Eur. Phys. J. C* **81**, 130 (2021)
- [6] S. Ozturk, *Adv. High Energy Phys* **2014**, 719216 (2014)
- [7] R. Sekhar Chivukula, E. H. Simmons, and N. Vignaroli, *Phys. Rev. D* **91**, 055019 (2015)
- [8] E. H. Simmons, R. S. Chivukula, P. Ittisamai *et al.*,
- [9] ATLAS Collaboration, *Phys. Rev. D* **87**, 012008 (2013)
- [10] ATLAS Collaboration, *JHEP* **12**, 086 (2012)
- [11] CMS Collaboration, *JHEP* **01**, 188 (2022)
- [12] CMS Collaboration, *Performance of quark/gluon discrimination using pp collision data at $\sqrt{s} = 8$ TeV*, CMS-PAS-JME-13-002, 2013
- [13] CMS Collaboration, *JHEP* **10**, 131 (2017)
- [14] CMS Collaboration, *JHEP* **05**, 090 (2013)
- [15] CMS Collaboration, *Eur. Phys. J. C* **77**, 467 (2017)

- [16] CMS Collaboration, *Phys. Rev. D* **98**, 092014 (2018)
- [17] CMS Collaboration, *JHEP* **11**, 113 (2018)
- [18] A. Altheimer *et al.*, *J. Phys. G* **39**, 063001 (2012)
- [19] J. R. Andersen *et al.*, *Les Houches 2015: Physics at TeV Colliders Standard Model Working Group Report*, 9th Les Houches Workshop on Physics at TeV Colliders, 2016, arXiv: 1605.04692[hep-ph]
- [20] A. J. Larkoski, J. Thaler, and W. J. Waalewijn, *JHEP* **11**, 129 (2014)
- [21] CDF Collaboration, *Phys. Rev. D* **71**, 112002 (2005)
- [22] OPAL Collaboration, *Eur. Phys. J. C* **11**, 217 (1999)
- [23] CLEO Collaboration, *Phys. Rev. D* **76**, 012005 (2007)
- [24] DELPHI Collaboration, *Phys. Lett. B* **449**, 383 (1999)
- [25] ZEUS Collaboration, *Nucl. Phys. B* **700**, 3 (2004)
- [26] ATLAS Collaboration, *Quark versus Gluon Jet Tagging Using Jet Images with the ATLAS Detector*, ATL-PHYS-PUB-2017-017, 2017
- [27] P. T. Komiske, E. M. Metodiev, and M. D. Schwartz, *JHEP* **01**, 110 (2017)
- [28] G. Altarelli and G. Parisi, *Nucl. Phys. B* **126**, 298 (1977)
- [29] C. Frye, A. J. Larkoski, J. Thaler *et al.*, *JHEP* **09**, 083 (2017)
- [30] J. Gallicchio and M. D. Schwartz, *Phys. Rev. Lett.* **107**, 172001 (2011)
- [31] J. Gallicchio and M. D. Schwartz, *JHEP* **04**, 090 (2013)
- [32] P. Gras *et al.*, *JHEP* **07**, 091 (2017)
- [33] P. T. Komiske, E. M. Metodiev, and J. Thaler, *JHEP* **11**, 059 (2018)
- [34] ATLAS Collaboration, *Eur. Phys. J. C* **74**, 3023 (2014)
- [35] ATLAS Collaboration, *Quark versus Gluon Jet Tagging Using Charged-Particle Constituent Multiplicity with the ATLAS Detector*, ATL-PHYS-PUB-2017-009, 2017
- [36] ATLAS Collaboration, *JINST* **3**, S08003 (2008)
- [37] B. Abbott *et al.*, *JINST* **13**, T05008 (2018)
- [38] ATLAS Collaboration, *Eur. Phys. J. C* **77**, 317 (2017)
- [39] ATLAS Collaboration, *The ATLAS Collaboration Software and Firmware*, ATL-SOFT-PUB-2021-001, 2021
- [40] ATLAS Collaboration, *Luminosity determination in pp collisions at $\sqrt{s} = 13$ TeV using the ATLAS detector at the LHC*, (2022), arXiv: 2212.09379[hep-ex]
- [41] ATLAS Collaboration, *JINST* **15**, P04003 (2020)
- [42] T. Sjöstrand *et al.*, *Comput. Phys. Commun.* **191**, 159 (2015)
- [43] NNPDF Collaboration, *Nucl. Phys. B* **867**, 244 (2013)
- [44] ATLAS Collaboration, *ATLAS Pythia 8 tunes to 7 TeV data*, ATL-PHYS-PUB-2014-021, 2014
- [45] ATLAS Collaboration, *Eur. Phys. J. C* **76**, 322 (2016)
- [46] ATLAS Collaboration, *Discrimination between Light Quark and Gluon Jets in pp collisions at $\sqrt{s} = 8$ TeV with the ATLAS Detector*, ATLAS-CONF-2016-034, 2016
- [47] ATLAS Collaboration, *Multijet simulation for 13 TeV ATLAS Analyses*, ATL-PHYS-PUB-2019-017, 2019
- [48] E. Bothmann *et al.*, *SciPost Phys.* **7**, 034 (2019)
- [49] S. Schumann and F. Krauss, *JHEP* **03**, 038 (2008)
- [50] S. Dulat *et al.*, *Phys. Rev. D* **93**, 033006 (2016)
- [51] J. C. Winter, F. Krauss, and G. Soff, *Eur. Phys. J. C* **36**, 381 (2004)
- [52] T. Sjöstrand, S. Mrenna, and P. Skands, *JHEP* **05**, 026 (2006)
- [53] J. Bellm *et al.*, *Eur. Phys. J. C* **76**, 196 (2016)
- [54] L. A. Harland-Lang, A. D. Martin, P. Motylinski *et al.*, *Eur. Phys. J. C* **75**, 204 (2015)
- [55] P. Nason, *JHEP* **11**, 040 (2004)
- [56] S. Frixione, P. Nason, and C. Oleari, *JHEP* **11**, 070 (2007)
- [57] S. Alioli, P. Nason, C. Oleari *et al.*, *JHEP* **06**, 043 (2010)
- [58] NNPDF Collaboration, *JHEP* **04**, 040 (2015)
- [59] M. Cacciari, G. P. Salam, and G. Soyez, *JHEP* **04**, 063 (2008)
- [60] ATLAS Collaboration, *Eur. Phys. J. C* **77**, 466 (2017)
- [61] ATLAS Collaboration, *Eur. Phys. J. C* **81**, 689 (2021)
- [62] ATLAS Collaboration, *Eur. Phys. J. C* **77**, 673 (2017)
- [63] M. Cacciari and G. P. Salam, *Phys. Lett. B* **659**, 119 (2008)
- [64] CDF Collaboration, *Phys. Rev. D* **78**, 072005 (2008)
- [65] ATLAS Collaboration, *Eur. Phys. J. C* **73**, 2676 (2013)
- [66] ATLAS Collaboration, *Eur. Phys. J. C* **73**, 2301 (2013)
- [67] ATLAS Collaboration, *Phys. Rev. D* **93**, 052003 (2016)
- [68] D. Krohn, M. D. Schwartz, T. Lin *et al.*, *Phys. Rev. Lett.* **110**, 212001 (2013)
- [69] I. Moul, L. Necib, and J. Thaler, *JHEP* **12**, 153 (2016)
- [70] A. J. Larkoski, G. P. Salam, and J. Thaler, *JHEP* **06**, 108 (2013)
- [71] G. Ke *et al.*, *LightGBM: A Highly Efficient Gradient Boosting Decision Tree*, *Advances in Neural Information Processing Systems* 30 (NIPS 2017), Curran Associates, Inc.,
- [72] T. Akiba, S. Sano, T. Yanase *et al.*, *Optuna: A Next-generation Hyperparameter Optimization Framework*, 2019, arXiv: 1907.10902[cs.LG]
- [73] ATLAS Collaboration, *Phys. Rev. D* **96**, 072002 (2017)
- [74] A. Buckley *et al.*, *Eur. Phys. J. C* **75**, 132 (2015)
- [75] S. Mrenna and P. Skands, *Phys. Rev. D* **94**, 074005 (2016)
- [76] ATLAS Collaboration, *ATLAS Computing Acknowledgements*, ATL-SOFT-PUB-2023-001, 2023

G. Aad¹⁰²  B. Abbott¹²⁰  K. Abeling⁵⁵  N.J. Abicht⁴⁹  S.H. Abidi²⁹  A. Aboulhorma^{35e} 
H. Abramowicz¹⁵¹  H. Abreu¹⁵⁰  Y. Abulaiti¹¹⁷  B.S. Acharya^{69a,69b,e}  C. Adam Bourdarios⁴ 
L. Adamczyk^{86a}  S.V. Addepalli²⁶  M.J. Addison¹⁰¹  J. Adelman¹¹⁵  A. Adiguzel^{21c}  T. Adye¹³⁴ 
A.A. Affolder¹³⁶  Y. Afik³⁶  M.N. Agaras¹³  J. Agarwala^{73a,73b}  A. Aggarwal¹⁰⁰  C. Agheorghiesei^{27c} 
A. Ahmad³⁶  F. Ahmadov^{38,ak}  W.S. Ahmed¹⁰⁴  S. Ahuja⁹⁵  X. Ai^{62a}  G. Aielli^{76a,76b}  A. Aikot¹⁶³ 
M. Ait Tamliah^{35e}  B. Aitbenchikh^{35a}  I. Aizenberg¹⁶⁹  M. Akbiyik¹⁰⁰  T.P.A. Åkesson⁹⁸  A.V. Akimov³⁷ 
D. Akiyama¹⁶⁸  N.N. Akolkar²⁴  K. Al Khoury⁴¹  G.L. Alberghi^{23b}  J. Albert¹⁶⁵  P. Albicocco⁵³ 
G.L. Albouy⁶⁰  S. Alderweireldt⁵²  M. Aleksa³⁶  I.N. Aleksandrov³⁸  C. Alexa^{27b}  T. Alexopoulos¹⁰ 
F. Alfonsi^{23b}  M. Algren⁵⁶  M. Alhroob¹²⁰  B. Ali¹³²  H.M.J. Ali⁹¹  S. Ali¹⁴⁸  S.W. Alibocus⁹² 
M. Aliev¹⁴⁵  G. Alimonti^{71a}  W. Alkahi⁵⁵  C. Allaire⁶⁶  B.M.M. Allbrooke¹⁴⁶  J.F. Allen⁵² 

C.A. Allendes Flores^{137f} P.P. Allport²⁰ A. Aloisio^{72a,72b} F. Alonso⁹⁰ C. Alpigiani¹³⁸
M. Alvarez Estevez⁹⁹ A. Alvarez Fernandez¹⁰⁰ M. Alves Cardoso⁵⁶ M.G. Alviggi^{72a,72b} M. Aly¹⁰¹
Y. Amaral Coutinho^{83b} A. Ambler¹⁰⁴ C. Amelung³⁶ M. Amerl¹⁰¹ C.G. Ames¹⁰⁹ D. Amidei¹⁰⁶
S.P. Amor Dos Santos^{130a} K.R. Amos¹⁶³ V. Ananiev¹²⁵ C. Anastopoulos¹³⁹ T. Andeen¹¹ J.K. Anders³⁶
S.Y. Andreev^{47a,47b} A. Andreazza^{71a,71b} S. Angelidakis⁹ A. Angerami^{41,ao} A.V. Anisenkov³⁷
A. Annovi^{74a} C. Antel⁵⁶ M.T. Anthony¹³⁹ E. Antipov¹⁴⁵ M. Antonelli⁵³ F. Anulli^{75a} M. Aoki⁸⁴
T. Aoki¹⁵³ J.A. Aparisi Pozo¹⁶³ M.A. Aparo¹⁴⁶ L. Aperio Bella⁴⁸ C. Appelt¹⁸ A. Apyan²⁶
N. Aranzabal³⁶ S.J. Arbiol Val⁸⁷ C. Arcangeletti⁵³ A.T.H. Arce⁵¹ E. Arena⁹² J-F. Arguin¹⁰⁸
S. Argyropoulos⁵⁴ J.-H. Arling⁴⁸ O. Arnaez⁴ H. Arnold¹¹⁴ G. Artoni^{75a,75b} H. Asada¹¹¹ K. Asai¹¹⁸
S. Asai¹⁵³ N.A. Asbah⁶¹ J. Assahsah^{35d} K. Assamagan²⁹ R. Astalos^{28a} S. Atashi¹⁶⁰ R.J. Atkin^{33a}
M. Atkinson¹⁶² H. Atmani^{35f} P.A. Atmasiddha¹⁰⁶ K. Augsten¹³² S. Auricchio^{72a,72b} A.D. Auriol²⁰
V.A. Austrup¹⁰¹ G. Avolio³⁶ K. Axiotis⁵⁶ G. Azuelos^{108,aw} D. Babal^{28b} H. Bachacou¹³⁵
K. Bachas^{152,w} A. Bachi³⁴ F. Backman^{47a,47b} A. Badea⁶¹ P. Bagnaia^{75a,75b} M. Bahmani¹⁸
A.J. Bailey¹⁶³ V.R. Bailey¹⁶² J.T. Baines¹³⁴ L. Baines⁹⁴ O.K. Baker¹⁷² E. Bakos¹⁵
D. Bakshi Gupta⁸ V. Balakrishnan¹²⁰ R. Balasubramanian¹¹⁴ E.M. Baldin³⁷ P. Balek^{86a}
E. Ballabene^{23b,23a} F. Balli¹³⁵ L.M. Baltes^{63a} W.K. Balunas³² J. Balz¹⁰⁰ E. Banas⁸⁷
M. Bandieramonte¹²⁹ A. Bandyopadhyay²⁴ S. Bansal²⁴ L. Barak¹⁵¹ M. Barakat⁴⁸ E.L. Barberio¹⁰⁵
D. Barberis^{57b,57a} M. Barbero¹⁰² M.Z. Barel¹¹⁴ K.N. Barends^{33a} T. Barillari¹¹⁰ M.-S. Barisits³⁶
T. Barklow¹⁴³ P. Baron¹²² D.A. Baron Moreno¹⁰¹ A. Baroncelli^{62a} G. Barone²⁹ A.J. Barr¹²⁶
J.D. Barr⁹⁶ L. Barranco Navarro^{47a,47b} F. Barreiro⁹⁹ J. Barreiro Guimarães da Costa^{14a} U. Barron¹⁵¹
M.G. Barros Teixeira^{130a} S. Barsov³⁷ F. Bartels^{63a} R. Bartoldus¹⁴³ A.E. Barton⁹¹ P. Bartos^{28a}
A. Basan^{100,af} M. Baselga⁴⁹ A. Bassalat^{66,b} M.J. Basso^{156a} C.R. Basson¹⁰¹ R.L. Bates⁵⁹
S. Batlamous^{35e} J.R. Batley³² B. Batool¹⁴¹ M. Battaglia¹³⁶ D. Battulga¹⁸ M. Baucé^{75a,75b} M. Bauer³⁶
P. Bauer²⁴ L.T. Bazzano Hurrell³⁰ J.B. Beacham⁵¹ T. Beau¹²⁷ J.Y. Beaucamp⁹⁰ P.H. Beauchemin¹⁵⁸
F. Becherer⁵⁴ P. Bechtel²⁴ H.P. Beck^{19,u} K. Becker¹⁶⁷ A.J. Beddall⁸² V.A. Bednyakov³⁸
C.P. Bee¹⁴⁵ L.J. Beamster¹⁵ T.A. Beermann³⁶ M. Begalli^{83d} M. Begel²⁹ A. Behera¹⁴⁵ J.K. Behr⁴⁸
J.F. Beirer⁵⁵ F. Beisiegel²⁴ M. Belfkir¹⁵⁹ G. Bella¹⁵¹ L. Bellagamba^{23b} A. Bellerive³⁴ P. Bellos²⁰
K. Beloborodov³⁷ D. Benchevkroun^{35a} F. Bendebba^{35a} Y. Benhammou¹⁵¹ M. Benoit²⁹ J.R. Bensinger²⁶
S. Bentvelsen¹¹⁴ L. Beresford⁴⁸ M. Beretta⁵³ E. Bergeaas Kuutmann¹⁶¹ N. Berger⁴ B. Bergmann¹³²
J. Beringer^{17a} G. Bernardi⁵ C. Bernius¹⁴³ F.U. Bernlochner²⁴ F. Bernon^{36,102} A. Berrocal Guardia¹³
T. Berry⁹⁵ P. Berta¹³³ A. Berthold⁵⁰ I.A. Bertram⁹¹ S. Bethke¹¹⁰ A. Betti^{75a,75b} A.J. Bevan⁹⁴
N.K. Bhalla⁵⁴ M. Bhamjee^{33c} S. Bhatta¹⁴⁵ D.S. Bhattacharya¹⁶⁶ P. Bhattarai¹⁴³ V.S. Bhopatkar¹²¹
R. Bi^{29,az} R.M. Bianchi¹²⁹ G. Bianco^{23b,23a} O. Biebel¹⁰⁹ R. Bielski¹²³ M. Biglietti^{77a} M. Bindi⁵⁵
A. Bingul^{21b} C. Bini^{75a,75b} A. Biondini⁹² C.J. Birch-sykes¹⁰¹ G.A. Bird^{20,134} M. Birman¹⁶⁹
M. Biros¹³³ S. Biryukov¹⁴⁶ T. Bisanz⁴⁹ E. Bisceglie^{43b,43a} J.P. Biswal¹³⁴ D. Biswas¹⁴¹ A. Bitadze¹⁰¹
K. Bjørke¹²⁵ I. Bloch⁴⁸ C. Blocker²⁶ A. Blue⁵⁹ U. Blumenschein⁹⁴ J. Blumenthal¹⁰⁰
G.J. Bobbink¹¹⁴ V.S. Bobrovnikov³⁷ M. Boehler⁵⁴ B. Boehm¹⁶⁶ D. Bogavac³⁶ A.G. Bogdanchikov³⁷
C. Boehm^{47a} V. Boisvert⁹⁵ P. Bokan⁴⁸ T. Bold^{86a} M. Bomben⁵ M. Bona⁹⁴ M. Boonekamp¹³⁵
C.D. Booth⁹⁵ A.G. Borbély^{59,at} I.S. Bordulev³⁷ H.M. Borecka-Bielska¹⁰⁸ G. Borissov⁹¹
D. Bortoletto¹²⁶ D. Boscherini^{23b} M. Bosman¹³ J.D. Bossio Sola³⁶ K. Bouaouda^{35a} N. Bouchhar¹⁶³
J. Boudreau¹²⁹ E.V. Bouhova-Thacker⁹¹ D. Boumediene⁴⁰ R. Bouquet¹⁶⁵ A. Boveia¹¹⁹ J. Boyd³⁶
D. Boye²⁹ I.R. Boyko³⁸ J. Bracini²⁰ N. Brahimi^{62d} G. Brandt¹⁷¹ O. Brandt³² F. Braren⁴⁸
B. Brau¹⁰³ J.E. Brau¹²³ R. Brenner¹⁶⁹ L. Brenner¹¹⁴ R. Brenner¹⁶¹ S. Bressler¹⁶⁹ D. Britton⁵⁹
D. Britzger¹¹⁰ I. Brock²⁴ G. Brooijmans⁴¹ W.K. Brooks^{137f} E. Brost²⁹ L.M. Brown^{165,n}
L.E. Bruce⁶¹ T.L. Bruckler¹²⁶ P.A. Bruckman de Renstrom⁸⁷ B. Brüers⁴⁸ A. Bruni^{23b} G. Bruni^{23b}
M. Bruschi^{23b} N. Bruscino^{75a,75b} T. Buanes¹⁶ Q. Buat¹³⁸ D. Buchin¹¹⁰ A.G. Buckley⁵⁹ O. Bulekov³⁷

A. Di Domenico^{75a,75b} C. Di Donato^{72a,72b} A. Di Girolamo³⁶ G. Di Gregorio³⁶ A. Di Luca^{78a,78b}
B. Di Micco^{77a,77b} R. Di Nardo^{77a,77b} C. Diaconu¹⁰² M. Diamantopoulou³⁴ F.A. Dias¹¹⁴
T. Dias Do Vale¹⁴² M.A. Diaz^{137a,137b} F.G. Diaz Capriles²⁴ M. Didenko¹⁶³ E.B. Diehl¹⁰⁶ L. Diehl⁵⁴
S. Díez Cornell⁴⁸ C. Díez Pardo¹⁴¹ C. Dimitriadis^{161,24,161} A. Dimitrievska^{17a} J. Dingfelder²⁴
I.-M. Dinu^{27b} S.J. Dittmeier^{63b} F. Dittus³⁶ F. Djama¹⁰² T. Djobava^{149b} J.I. Djuvsland¹⁶
C. Doglioni^{101,98} A. Dohnalova^{28a} J. Dolejsi¹³³ Z. Dolezal¹³³ K.M. Dona³⁹ M. Donadelli^{83c}
B. Dong¹⁰⁷ J. Donini⁴⁰ A. D'Onofrio^{77a,77b} M. D'Onofrio⁹² J. Dopke¹³⁴ A. Doria^{72a}
N. Dos Santos Fernandes^{130a} P. Dougan¹⁰¹ M.T. Dova⁹⁰ A.T. Doyle⁵⁹ M.A. Dragnet¹²⁶ E. Dreyer¹⁶⁹
I. Drivas-koulouris¹⁰ M. Drnevich¹¹⁷ A.S. Drobac¹⁵⁸ M. Drozdova⁵⁶ D. Du^{62a} T.A. du Pree¹¹⁴
F. Dubinin³⁷ M. Dubovskiy^{28a} E. Duchovni¹⁶⁹ G. Duckeck¹⁰⁹ O.A. Ducu^{27b} D. Duda⁵² A. Dudarev³⁶
E.R. Duden²⁶ M. D'uffizi¹⁰¹ L. Duflost⁶⁶ M. Dührssen³⁶ C. Dülsen¹⁷¹ A.E. Dumitriu^{27b}
M. Dunford^{63a} S. Dungs⁴⁹ K. Dunne^{47a,47b} A. Duperrin¹⁰² H. Duran Yildiz^{3a} M. Düren⁵⁸
A. Durglishvili^{149b} B.L. Dwyer¹¹⁵ G.I. Dyckes^{17a} M. Dyndal^{86a} B.S. Dziedzic⁸⁷ Z.O. Earnshaw¹⁴⁶
G.H. Eberwein¹²⁶ B. Eckerova^{28a} S. Eggebrecht⁵⁵ E. Egidio Purcino De Souza¹²⁷ L.F. Ehrke⁵⁶
G. Eigen¹⁶ K. Einsweiler^{17a} T. Ekelof⁶¹ P.A. Ekman⁹⁸ S. El Farkh^{35b} Y. El Ghazali^{35b}
H. El Jarrari^{35e,148} A. El Moussaouy^{108,ab} V. Ellajosyula¹⁶¹ M. Ellert¹⁶¹ F. Ellinghaus¹⁷¹ N. Ellis³⁶
J. Elmsheuser²⁹ M. Elsing³⁶ D. Emeliyanov¹³⁴ Y. Enari¹⁵³ I. Ene^{17a} S. Epari¹³ J. Erdmann⁴⁹
P.A. Erland⁸⁷ M. Errenst¹⁷¹ M. Escalier⁶⁶ C. Escobar¹⁶³ E. Etzion¹⁵¹ G. Evans^{130a} H. Evans⁶⁸
L.S. Evans⁹⁵ M.O. Evans¹⁴⁶ A. Ezhilov³⁷ S. Ezzarqtouni^{35a} F. Fabbri⁵⁹ L. Fabbri^{23b,23a} G. Facini⁹⁶
V. Fadeyev¹³⁶ R.M. Fakhrutdinov³⁷ S. Falciano^{75a} L.F. Falda Ulhoa Coelho³⁶ P.J. Falke²⁴ J. Faltova¹³³
C. Fan¹⁶² Y. Fan^{14a} Y. Fang^{14a,14e} M. Fanti^{71a,71b} M. Faraj^{69a,69b} Z. Farazpay⁹⁷ A. Farbin⁸
A. Farilla^{77a} T. Farooque¹⁰⁷ S.M. Farrington⁵² F. Fassi^{35e} D. Fassouliotis⁹ M. Faucci Giannelli^{76a,76b}
W.J. Fawcett³² L. Fayard⁶⁶ P. Federic¹³³ P. Federicova¹³¹ O.L. Fedin^{37,a} G. Fedotov³⁷
M. Feickert¹⁷⁰ L. Feligioni¹⁰² D.E. Fellers¹²³ C. Feng^{62b} M. Feng^{14b} Z. Feng¹¹⁴ M.J. Fenton¹⁶⁰
A.B. Fenyuk³⁷ L. Ferencz⁴⁸ R.A.M. Ferguson⁹¹ S.I. Fernandez Luengo^{137f} P. Fernandez Martinez¹³
M.J.V. Fernoux¹⁰² J. Ferrando⁴⁸ A. Ferrari¹⁶¹ P. Ferrari^{114,113} R. Ferrari^{73a} D. Ferrere⁵⁶
C. Ferretti¹⁰⁶ F. Fiedler¹⁰⁰ P. Fiedler¹³² A. Filipčič⁹³ E.K. Filmer¹ F. Filthaut¹¹³
M.C.N. Fiolhais^{130a,130c,d} L. Fiorini¹⁶³ W.C. Fisher¹⁰⁷ T. Fitschen¹⁰¹ P.M. Fitzhugh¹³⁵ I. Fleck¹⁴¹
P. Fleischmann¹⁰⁶ T. Flick¹⁷¹ M. Flores^{33d,ap} L.R. Flores Castillo^{64a} L. Flores Sanz De Acedo³⁶
F.M. Follega^{78a,78b} N. Fomin¹⁶ J.H. Foo¹⁵⁵ B.C. Forland⁶⁸ A. Formica¹³⁵ A.C. Forti¹⁰¹ E. Fortin³⁶
A.W. Fortman⁶¹ M.G. Foti^{17a} L. Fountas⁹¹ D. Fournier⁶⁶ H. Fox⁹¹ P. Francavilla^{74a,74b}
S. Francescato⁶¹ S. Franchellucci⁵⁶ M. Franchini^{23b,23a} S. Franchino^{63a} D. Francis³⁶ L. Franco¹¹³
V. Franco Lima³⁶ L. Franconi⁴⁸ M. Franklin⁶¹ G. Frattari²⁶ A.C. Freegard⁹⁴ W.S. Freund^{83b}
Y.Y. Frid¹⁵¹ J. Friend⁵⁹ N. Fritzsche⁵⁰ A. Froch⁵⁴ D. Froidevaux³⁶ J.A. Frost¹²⁶ Y. Fu^{62a}
S. Fuenzalida Garrido^{137f} M. Fujimoto^{118,aq} E. Fullana Torregrosa^{163,*} K.Y. Fung^{64a}
E. Furtado De Simas Filho^{83b} M. Furukawa¹⁵³ J. Fuster¹⁶³ A. Gabrielli^{23b,23a} A. Gabrielli¹⁵⁵ P. Gadov³⁶
G. Gagliardi^{57b,57a} L.G. Gagnon^{17a} E.J. Gallas¹²⁶ B.J. Gallop¹³⁴ K.K. Gan¹¹⁹ S. Ganguly¹⁵³
Y. Gao⁵² F.M. Garay Walls^{137a,137b} B. Garcia^{29,az} C. García¹⁶³ A. Garcia Alonso¹¹⁴
A.G. Garcia Caffaro¹⁷² J.E. García Navarro¹⁶³ M. Garcia-Sciveres^{17a} G.L. Gardner¹²⁸ R.W. Gardner³⁹
N. Garelli¹⁵⁸ D. Garg⁸⁰ R.B. Garg^{143,u} J.M. Gargan⁵² C.A. Garner¹⁵⁵ C.M. Garvey^{33a} P. Gaspar^{83b}
V.K. Gassmann¹⁵⁸ G. Gaudio^{73a} V. Gautam¹³ P. Gauzzi^{75a,75b} I.L. Gavrilenko³⁷ A. Gavriluk³⁷
C. Gay¹⁶⁴ G. Gaycken⁴⁸ E.N. Gazis¹⁰ A.A. Geanta^{27b} C.M. Gee¹³⁶ C. Gemme^{57b} M.H. Genest⁶⁰
S. Gentile^{75a,75b} A.D. Gentry¹¹² S. George⁹⁵ W.F. George²⁰ T. Geralis⁴⁶ P. Gessinger-Befurt³⁶
M.E. Geyik¹⁷¹ M. Ghani¹⁶⁷ M. Ghneimat¹⁴¹ K. Ghorbanian⁹⁴ A. Ghosal¹⁴¹ A. Ghosh¹⁶⁰ A. Ghosh⁷
B. Giacobbe^{23b} S. Giagu^{75a,75b} T. Giani¹¹⁴ P. Giannetti^{74a} A. Giannini^{62a} S.M. Gibson⁹⁵
M. Gignac¹³⁶ D.T. Gil^{86b} A.K. Gilbert^{86a} B.J. Gilbert⁴¹ D. Gillberg³⁴ G. Gilles¹¹⁴













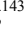
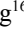




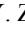
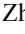



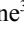
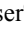
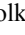
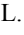
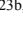
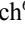
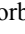
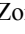
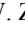
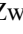
N.E.K. Gillwald⁴⁸ L. Ginabat¹²⁷ D.M. Gingrich^{2,aw} M.P. Giordani^{69a,69c} P.F. Giraud¹³⁵
 G. Giugliarelli^{69a,69c} D. Giugni^{71a} F. Giuliani³⁶ I. Gkialas^{9,1} L.K. Gladilin³⁷ C. Glasman⁹⁹
 G.R. Gledhill¹²³ G. Glemža⁴⁸ M. Glisic¹²³ I. Gnesi^{43b,g} Y. Go^{29,az} M. Goblirsch-Kolb³⁶ B. Gocke⁴⁹
 D. Godin¹⁰⁸ B. Gokturk^{21a} S. Goldfarb¹⁰⁵ T. Golling⁵⁶ M.G.D. Gololo^{33g} D. Golubkov³⁷
 J.P. Gombas¹⁰⁷ A. Gomes^{130a,130b} G. Gomes Da Silva¹⁴¹ A.J. Gomez Delegido¹⁶³ R. Gonçalo^{130a,130c}
 G. Gonella¹²³ L. Gonella²⁰ A. Gongadze^{149c} F. Gonnella²⁰ J.L. Gonski⁴¹ R.Y. González Andana⁵²
 S. González de la Hoz¹⁶³ S. Gonzalez Fernandez¹³ R. Gonzalez Lopez⁹² C. Gonzalez Renteria^{17a}
 M.V. Gonzalez Rodrigues⁴⁸ R. Gonzalez Suarez¹⁶¹ S. Gonzalez-Sevilla⁵⁶ G.R. Gonzalvo Rodriguez¹⁶³
 L. Goossens³⁶ B. Gorini³⁶ E. Gorini^{70a,70b} A. Gorišek⁹³ T.C. Gosart¹²⁸ A.T. Goshaw⁵¹
 M.I. Gostkin³⁸ S. Goswami¹²¹ C.A. Gottardo³⁶ S.A. Gotz¹⁰⁹ M. Gouighri^{35b} V. Goumarre⁴⁸
 A.G. Goussiou¹³⁸ N. Govender^{33c} I. Grabowska-Bold^{86a} K. Graham³⁴ E. Gramstad¹²⁵
 S. Grancagnolo^{70a,70b} M. Grandi¹⁴⁶ C.M. Grant^{1,135} P.M. Gravila^{27f} F.G. Gravili^{70a,70b} H.M. Gray^{17a}
 M. Greco^{70a,70b} C. Grefe²⁴ I.M. Gregor⁴⁸ P. Grenier¹⁴³ S.G. Grewe¹¹⁰ C. Grieco¹³ A.A. Grillo¹³⁶
 K. Grimm³¹ S. Grinstein^{13,ad} J.-F. Grivaz⁶⁶ E. Gross¹⁶⁹ J. Grosse-Knetter⁵⁵ C. Grud¹⁰⁶ J.C. Grundy¹²⁶
 L. Guan¹⁰⁶ W. Guan²⁹ C. Gubbels¹⁶⁴ J.G.R. Guerrero Rojas¹⁶³ G. Guerrieri^{69a,69c} F. Guescini¹¹⁰
 R. Gugel¹⁰⁰ J.A.M. Guhit¹⁰⁶ A. Guida¹⁸ T. Guillemain⁴ E. Guillonon^{167,134} S. Guindon³⁶ F. Guo^{14a,14c}
 J. Guo^{62c} L. Guo⁴⁸ Y. Guo¹⁰⁶ R. Gupta⁴⁸ R. Gupta¹²⁹ S. Gurbuz²⁴ S.S. Gurdasani⁵⁴
 G. Gustavoino³⁶ M. Guth⁵⁶ P. Gutierrez¹²⁰ L.F. Gutierrez Zagazeta¹²⁸ M. Gutsche⁵⁰ C. Gutschow⁹⁶
 C. Gwenlan¹²⁶ C.B. Gwilliam⁹² E.S. Haaland¹²⁵ A. Haas¹¹⁷ M. Habedank⁴⁸ C. Haber^{17a}
 H.K. Hadavand⁸ A. Hadel¹⁰⁰ S. Hadzic¹¹⁰ A.I. Hagan⁹¹ J.J. Hahn¹⁴¹ E.H. Haines⁹⁶ M. Haleem¹⁶⁶
 J. Haley¹²¹ J.J. Hall¹³⁹ G.D. Hallewell¹⁰² L. Halser¹⁹ K. Hamano¹⁶⁵ M. Hamer²⁴ G.N. Hamity⁵²
 E.J. Hampshire⁹⁵ J. Han^{62b} K. Han^{62a} L. Han^{14c} L. Han^{62a} S. Han^{17a} Y.F. Han¹⁵⁵ K. Hanagaki⁸⁴
 M. Hance¹³⁶ D.A. Hangal^{141,ao} H. Hanif⁴² M.D. Hank¹²⁸ R. Hankache¹⁰¹ J.B. Hansen⁴²
 J.D. Hansen⁴² P.H. Hansen⁴² K. Hara¹⁵⁷ D. Harada⁵⁶ T. Harenberg¹⁷¹ S. Harkusha³⁷
 M.L. Harris¹⁰³ Y.T. Harris¹²⁶ J. Harrison¹³ N.M. Harrison¹¹⁹ P.F. Harrison¹⁶⁷ N.M. Hartman¹¹⁰
 N.M. Hartman¹⁰⁹ Y. Hasegawa¹⁴⁰ R. Hauser¹⁰⁷ C.M. Hawkes²⁰ R.J. Hawkins³⁶ Y. Hayashi¹⁵³
 S. Hayashida¹¹¹ D. Hayden¹⁰⁷ C. Hayes¹⁰⁶ R.L. Hayes¹¹⁴ C.P. Hays¹²⁶ J.M. Hays⁹⁴ H.S. Hayward⁹²
 F. He^{62a} M. He^{14a,14c} Y. He¹⁵⁴ Y. He⁴⁸ N.B. Heatley⁹⁴ V. Hedberg⁹⁸ A.L. Heggelund¹²⁵
 N.D. Hehir⁹⁴ C. Heidegger⁵⁴ K.K. Heidegger⁵⁴ W.D. Heidorn⁸¹ J. Heilman³⁴ S. Heim⁴⁸
 T. Heim^{17a} J.G. Heinlein¹²⁸ J.J. Heinrich¹²³ L. Heinrich^{110,au} J. Hejbal¹³¹ L. Helary⁴⁸ A. Held¹⁷⁰
 S. Hellesund¹⁶ C.M. Helling¹⁶⁴ S. Hellman^{47a,47b} R.C.W. Henderson⁹¹ L. Henkelmann³² A.M. Henriques
 Correia³⁶ H. Herde⁹⁸ Y. Hernández Jiménez¹⁴⁵ L.M. Herrmann²⁴ T. Herrmann⁵⁰
 G. Herten⁵⁴ R. Hertenberger¹⁰⁹ L. Hervas³⁶ M.E. Hesping¹⁰⁰ N.P. Hesse^{156a} H. Hibi⁸⁵ E. Hill¹⁵⁵
 S.J. Hillier²⁰ J.R. Hinds¹⁰⁷ F. Hinterkeuser²⁴ M. Hirose¹²⁴ S. Hirose¹⁵⁷ D. Hirschbuehl¹⁷¹
 T.G. Hitchings¹⁰¹ B. Hiti⁹³ J. Hobbs¹⁴⁵ R. Hobincu^{27e} N. Hod¹⁶⁹ M.C. Hodgkinson¹³⁹
 B.H. Hodgkinson³² A. Hoecker³⁶ J. Hofer⁴⁸ T. Holm²⁴ M. Holzbock¹¹⁰ L.B.A.H. Hommels³²
 B.P. Honan¹⁰¹ J. Hong^{62c} T.M. Hong¹²⁹ B.H. Hooberman¹⁶² W.H. Hopkins⁶ Y. Horii¹¹¹ S. Hou¹⁴⁸
 A.S. Howard⁹³ J. Howarth⁵⁹ J. Hoya⁶ M. Hrabovsky¹²² A. Hrynevich⁴⁸ T. Hryn'ova⁴ P.J. Hsu⁶⁵
 S.-C. Hsu¹³⁸ Q. Hu^{62a} Y.F. Hu^{14a,14c} S. Huang^{64b} X. Huang^{14c} X. Huang^{14a,14c} Y. Huang^{139,m}
 Y. Huang^{14a} Z. Huang¹⁰¹ Z. Hubacek¹³² M. Huebner²⁴ F. Huegging²⁴ T.B. Huffman¹²⁶
 C.A. Hugli⁴⁸ M. Huhtinen³⁶ S.K. Huiberts¹⁶ R. Hulsken¹⁰⁴ N. Huseynov¹² J. Huston¹⁰⁷ J. Huth⁶¹
 R. Hyneman¹⁴³ G. Iacobucci⁵⁶ G. Iakovidis²⁹ I. Ibragimov¹⁴¹ L. Iconomidou-Fayard¹⁶⁶ P. Iengo^{72a,72b}
 R. Iguchi¹⁵³ T. Iizawa^{126,r} Y. Ikegami⁸⁴ N. Ilic¹⁵⁵ H. Imam^{35a} M. Ince Lezki⁵⁶ T. Ingebreten
 Carlson^{47a,47b} G. Introzzi^{73a,73b} M. Iodice^{77a} V. Ippolito^{75a,75b} R.K. Irwin⁹² M. Ishino¹⁵³ W. Islam¹⁷⁰
 C. Issever^{18,48} S. Istin^{21a,bb} H. Ito¹⁶⁸ J.M. Iturbe Ponce^{64a} R. Iuppa^{78a,78b} A. Ivina¹⁶⁹ J.M. Izen⁴⁵
 V. Izzo^{72a} P. Jacka^{131,132} P. Jackson¹ R.M. Jacobs⁴⁸ B.P. Jaeger¹⁴² C.S. Jagfeld¹⁰⁹ G. Jain^{156a}

P. Jain⁵⁴ ID, K. Jakobs⁵⁴ ID, T. Jakobek¹⁶⁹ ID, J. Jamieson⁵⁹ ID, K.W. Janas^{86a} ID, M. Javurkova¹⁰³ ID, F. Jeanneau¹³⁵ ID,
 L. Jeanty¹²³ ID, J. Jejelava^{149a,al} ID, P. Jenni^{54,i} ID, C.E. Jessiman³⁴ ID, S. Jézéquel⁴ ID, C. Jia^{62b}, J. Jia¹⁴⁵ ID, X. Jia⁶¹ ID,
 X. Jia^{14a,14c} ID, Z. Jia^{14c} ID, S. Jiggins⁴⁸ ID, J. Jimenez Pena¹³ ID, S. Jin^{14c} ID, A. Jinaru^{27b} ID, O. Jinnouchi¹⁵⁴ ID,
 P. Johansson¹³⁹ ID, K.A. Johns⁷ ID, J.W. Johnson¹³⁶ ID, D.M. Jones³² ID, E. Jones⁴⁸ ID, P. Jones³² ID, R.W.L. Jones⁹¹ ID,
 T.J. Jones⁹² ID, H.L. Joos^{55,36} ID, R. Joshi¹¹⁹ ID, J. Jovicevic¹⁵ ID, X. Ju^{17a} ID, J.J. Junggeburth^{103,v} ID, T. Junkermann^{63a} ID,
 A. Juste Rozas^{13,ad} ID, M.K. Juzek⁸⁷ ID, S. Kabana^{137e} ID, A. Kaczmarek⁸⁷ ID, M. Kado¹¹⁰ ID, H. Kagan¹¹⁹ ID,
 M. Kagan¹⁴³ ID, A. Kahn⁴¹, A. Kahn¹²⁸ ID, C. Kahra¹⁰⁰ ID, T. Kaji¹⁵³ ID, E. Kajomovitz¹⁵⁰ ID, N. Kakati¹⁶⁹ ID,
 I. Kalaitzidou⁵⁴ ID, C.W. Kalderon²⁹ ID, A. Kamenshchikov¹⁵⁵ ID, N.J. Kang¹³⁶ ID, D. Kar^{33g} ID, K. Karava¹²⁶ ID,
 M.J. Kareem^{156b} ID, E. Karentzos⁵⁴ ID, I. Karkanias¹⁵² ID, O. Karkout¹¹⁴ ID, S.N. Karpov³⁸ ID, Z.M. Karpova³⁸ ID,
 V. Kartvelishvili⁹¹ ID, A.N. Karyukhin³⁷ ID, E. Kasimi¹⁵² ID, J. Katzy⁴⁸ ID, S. Kaur³⁴ ID, K. Kawade¹⁴⁰ ID,
 M.P. Kawale¹²⁰ ID, C. Kawamoto⁸⁸ ID, T. Kawamoto¹³⁵ ID, E.F. Kay³⁶ ID, F.I. Kaya¹⁵⁸ ID, S. Kazakos¹⁰⁷ ID,
 V.F. Kazanin³⁷ ID, Y. Ke¹⁴⁵ ID, J.M. Keaveney^{33a} ID, R. Keeler¹⁶⁵ ID, G.V. Kehris⁶¹ ID, J.S. Keller³⁴ ID, A.S. Kelly⁹⁶,
 J.J. Kempster¹⁴⁶ ID, K.E. Kennedy⁴¹ ID, P.D. Kennedy¹⁰⁰ ID, O. Kepka¹³¹ ID, B.P. Kerridge¹⁶⁷ ID, S. Kersten¹⁷¹ ID,
 B.P. Kerševan⁹³ ID, S. Keshri⁶⁶ ID, L. Keszeghova^{28a} ID, S. Ketabchi Haghighat¹⁵⁵ ID, R.A. Khan¹²⁹, M. Khandoga¹²⁷ ID,
 A. Khanov¹²¹ ID, A.G. Kharlamov³⁷ ID, T. Kharlamova³⁷ ID, E.E. Khoda¹³⁸ ID, M. Kholodenko³⁷ ID, T.J. Khoo¹⁸ ID,
 G. Khoriali¹⁶⁶ ID, J. Khubua^{149b} ID, Y.A.R. Khwaira⁶⁶ ID, A. Kilgallon¹²³ ID, D.W. Kim^{47a,47b} ID, Y.K. Kim³⁹ ID,
 N. Kimura⁹⁶ ID, M.K. Kingston⁵⁵ ID, A. Kirchhoff⁵⁵ ID, C. Kirfel²⁴ ID, F. Kirfel²⁴ ID, J. Kirk¹³⁴ ID, A.E. Kiryunin¹¹⁰ ID,
 C. Kitsaki¹⁰ ID, O. Kivernyk²⁴ ID, M. Klassen^{63a} ID, C. Klein³⁴ ID, L. Klein¹⁶⁶ ID, M.H. Klein¹⁰⁶ ID, M. Klein⁹² ID,
 S.B. Klein⁵⁶ ID, U. Klein⁹² ID, P. Klimek³⁶ ID, A. Klimentov²⁹ ID, T. Klioutchnikova³⁶ ID, P. Kluit¹¹⁴ ID, S. Kluth¹¹⁰ ID,
 E. Kneringer⁷⁹ ID, T.M. Knight¹⁵⁵ ID, A. Knue⁴⁹ ID, R. Kobayashi⁸⁸ ID, D. Kobylanski¹⁶⁹ ID, S.F. Koch¹²⁶ ID,
 M. Kocian¹⁴³ ID, P. Kodyš¹³³ ID, D.M. Koeck¹²³ ID, P.T. Koendig²⁴ ID, T. Koffas³⁴ ID, M. Kolb¹³⁵ ID, I. Koletsou⁴ ID,
 T. Komarek¹²² ID, K. Köneke⁵⁴ ID, A.X.Y. Kong¹ ID, T. Kono¹¹⁸ ID, N. Konstantinidis⁹⁶ ID, P. Kontaxakis⁵⁶ ID,
 B. Konya⁹⁸ ID, R. Kopeliansky⁶⁸ ID, S. Koperny^{86a} ID, K. Korcyl⁸⁷ ID, K. Kordas^{152,f} ID, G. Koren¹⁵¹ ID, A. Korn⁹⁶ ID,
 S. Korn⁵⁵ ID, I. Korolkov¹³ ID, N. Korotkova³⁷ ID, B. Kortman¹¹⁴ ID, O. Kortner¹¹⁰ ID, S. Kortner¹¹⁰ ID,
 W.H. Kostecka¹¹⁵ ID, V.V. Kostyukhin¹⁴¹ ID, A. Kotschechagia¹³⁵ ID, A. Kotwal⁵¹ ID, A. Koulouris³⁶ ID,
 A. Kourkouveli-Charalampidi^{73a,73b} ID, C. Kourkouvelis⁹ ID, E. Kourlitis^{110,au} ID, O. Kovanda¹⁴⁶ ID, R. Kowalewski¹⁶⁵ ID,
 W. Kozanecki¹³⁵ ID, A.S. Kozhin³⁷ ID, V.A. Kramarenko³⁷ ID, G. Kramberger⁹³ ID, P. Kramer¹⁰⁰ ID, M.W. Krasny¹²⁷ ID,
 A. Krasznahorkay³⁶ ID, J.W. Kraus¹⁷¹ ID, J.A. Kremer⁴⁸ ID, T. Kresse⁵⁰ ID, J. Kretschmar⁹² ID, K. Kreul¹⁸ ID,
 P. Krieger¹⁵⁵ ID, S. Krishnamurthy¹⁰³ ID, M. Krivos¹³³ ID, K. Krizka²⁰ ID, K. Kroeninger⁴⁹ ID, H. Kroha¹¹⁰ ID,
 J. Kroll¹³¹ ID, J. Kroll¹²⁸ ID, K.S. Krowpman¹⁰⁷ ID, U. Kruchonak³⁸ ID, H. Krüger²⁴ ID, N. Krumnack⁸¹, M.C. Kruse⁵¹ ID,
 J.A. Krzysiak⁸⁷ ID, O. Kuchinskaia³⁷ ID, S. Kuday^{3a} ID, S. Kuehn³⁶ ID, R. Kuesters⁵⁴ ID, T. Kuhl⁴⁸ ID, V. Kukhtin³⁸ ID,
 Y. Kulchitsky^{37,a} ID, S. Kuleshov^{137d,137b} ID, M. Kumar^{33g} ID, N. Kumari⁴⁸ ID, A. Kupco¹³¹ ID, T. Kupfer⁴⁹,
 A. Kupich³⁷ ID, O. Kuprash⁵⁴ ID, H. Kurashige⁸⁵ ID, L.L. Kurchaninov^{156a} ID, O. Kurdys⁶⁶ ID, Y.A. Kurochkin³⁷ ID,
 A. Kurova³⁷ ID, M. Kuze¹⁵⁴ ID, A.K. Kvam¹⁰³ ID, J. Kvita¹²² ID, T. Kwan¹⁰⁴ ID, N.G. Kyriacou¹⁰⁶ ID, L.A.O. Laatu¹⁰² ID,
 C. Lacasta¹⁶³ ID, F. Lacava^{75a,75b} ID, H. Lacker¹⁸ ID, D. Lacour¹²⁷ ID, N.N. Lad⁹⁶ ID, E. Ladygin³⁸ ID, B. Laforge¹²⁷ ID,
 T. Lagouri^{137e} ID, F.Z. Lahbabi^{35a} ID, S. Lai⁵⁵ ID, I.K. Lakomicc^{86a} ID, N. Lalloue⁶⁰ ID, J.E. Lambert^{165,n} ID,
 S. Lammers⁶⁸ ID, W. Lampl⁷ ID, C. Lampoudis^{152,f} ID, A.N. Lancaster¹¹⁵ ID, E. Lançon²⁹ ID, U. Landgraf⁵⁴ ID,
 M.P.J. Landon⁹⁴ ID, V.S. Lang⁵⁴ ID, R.J. Langenberg¹⁰³ ID, O.K.B. Langrekken¹²⁵ ID, A.J. Lankford¹⁶⁰ ID, F. Lanni³⁶ ID,
 K. Lantzsck²⁴ ID, A. Lanza^{73a} ID, A. Lapertosa^{57b,57a} ID, J.F. Laporte¹³⁵ ID, T. Lari^{71a} ID, F. Lasagni Manghi^{23b} ID,
 M. Lassnig³⁶ ID, V. Latonova¹³¹ ID, A. Laudrain¹⁰⁰ ID, A. Laurier¹⁵⁰ ID, S.D. Lawlor¹³⁹ ID, Z. Lawrence¹⁰¹ ID,
 M. Lazzaroni^{71a,71b} ID, B. Le¹⁰¹, E.M. Le Boulicaut⁵¹ ID, B. Leban⁹³ ID, A. Lebedev⁸¹ ID, M. LeBlanc^{101,as} ID,
 F. Ledroit-Guillon⁶⁰ ID, A.C.A. Lee⁹⁶, S.C. Lee¹⁴⁸ ID, S. Lee^{47a,47b} ID, T.F. Lee⁹² ID, L.L. Leeuw^{33c} ID, H.P. Lefebvre⁹⁵ ID,
 M. Lefebvre¹⁶⁵ ID, C. Leggett^{17a} ID, G. Lehmann Miotto³⁶ ID, M. Leigh⁵⁶ ID, W.A. Leight¹⁰³ ID, W. Leinonen¹¹³ ID,
 A. Leisos^{152,ac} ID, M.A.L. Leite^{83c} ID, C.E. Leitgeb⁴⁸ ID, R. Leitner¹³³ ID, K.J.C. Leney⁴⁴ ID, T. Lenz²⁴ ID, S. Leone^{74d} ID,
 C. Leonidopoulos⁵² ID, A. Leopold¹⁴⁴ ID, C. Leroy¹⁰⁸ ID, R. Les¹⁰⁷ ID, C.G. Lester³² ID, M. Levchenko³⁷ ID,
 J. Levêque⁴ ID, D. Levin¹⁰⁶ ID, L.J. Levinson¹⁶⁹ ID, M.P. Lewicki⁸⁷ ID, D.J. Lewis⁴ ID, A. Li⁵ ID, B. Li^{62b} ID

C. Li^{62a} C-Q. Li^{62c} H. Li^{62a} H. Li^{62b} H. Li^{14c} H. Li^{14b} H. Li^{62b} J. Li^{62c} K. Li¹³⁸ L. Li^{62c}
M. Li^{14a,14e} Q.Y. Li^{62a} S. Li^{14a,14e} S. Li^{62d,62c,e} T. Li^{5,c} X. Li¹⁰⁴ Z. Li¹²⁶ Z. Li¹⁰⁴ Z. Li⁹²
Z. Li^{14a,14e} S. Liang^{14a,14e} Z. Liang^{14a} M. Liberatore^{135,am} B. Liberti^{76a} K. Lie^{64c} J. Lieber Marin^{83b}
H. Lien⁶⁸ K. Lin¹⁰⁷ R.E. Lindley⁷ J.H. Lindon² E. Lipeles¹²⁸ A. Lipniacka¹⁶ A. Lister¹⁶⁴
J.D. Little⁴ B. Liu^{14a} B.X. Liu¹⁴² D. Liu^{62d,62c} J.B. Liu^{62a} J.K.K. Liu³² K. Liu^{62d,62c} M. Liu^{62a}
M.Y. Liu^{62a} P. Liu^{14a} Q. Liu^{62d,138,62c} X. Liu^{62a} Y. Liu^{14d,14e} Y.L. Liu^{62b} Y.W. Liu^{62a}
J. Llorente Merino¹⁴² S.L. Lloyd⁹⁴ E.M. Lobodzinska⁴⁸ P. Loch⁷ T. Lohse¹⁸ K. Lohwasser¹³⁹
E. Loiacono⁴⁸ M. Lokajicek^{131,*} J.D. Lomas²⁰ J.D. Long¹⁶² I. Longarini¹⁶⁰ L. Longo^{70a,70b}
R. Longo¹⁶² I. Lopez Paz⁶⁷ A. Lopez Solis⁴⁸ J. Lorenz¹⁰⁹ N. Lorenzo Martinez⁴ A.M. Lory¹⁰⁹
O. Loseva³⁷ X. Lou^{47a,47b} X. Lou^{14a,14e} A. Lounis⁶⁶ J. Love⁶ P.A. Love⁹¹ G. Lu^{14a,14e} M. Lu⁸⁰
S. Lu¹²⁸ Y.J. Lu⁶⁵ H.J. Lubatti¹³⁸ C. Luci^{75a,75b} F.L. Lucio Alves^{14c} A. Lucotte⁶⁰ F. Luehring⁶⁸
I. Luise¹⁴⁵ O. Lukianchuk⁶⁶ O. Lundberg¹⁴⁴ B. Lund-Jensen¹⁴⁴ N.A. Luongo¹²³ M.S. Lutz¹⁵¹
A.B. Lux²⁵ D. Lynn²⁹ H. Lyons⁹² R. Lysak¹³¹ E. Lytken⁹⁸ V. Lyubushkin³⁸ T. Lyubushkina³⁸
M.M. Lyukova¹⁴⁵ H. Ma²⁹ K. Ma^{62a} L.L. Ma^{62b} Y. Ma¹²¹ D.M. Mac Donell¹⁶⁵ G. Maccarrone⁵³
J.C. MacDonald¹⁰⁰ P.C. Machado De Abreu Farias^{83b} R. Madar⁴⁰ W.F. Mader⁵⁰ T. Madula⁹⁶
J. Maeda⁸⁵ T. Maeno²⁹ H. Maguire¹³⁹ V. Maiboroda¹³⁵ A. Maio^{130a,130b,130d} K. Maj^{86a}
O. Majersky⁴⁸ S. Majewski¹²³ N. Makovec⁶⁶ V. Maksimovic¹⁵ B. Malaescu¹²⁷ Pa. Malecki⁸⁷
V.P. Maleev³⁷ F. Malek⁶⁰ M. Mali⁹³ D. Malito^{95,s} U. Mallik⁸⁰ S. Maltezos¹⁰ S. Malyukov³⁸
J. Mamuzic¹³ G. Mancini⁵³ G. Manco^{73a,73b} J.P. Mandalia⁹⁴ I. Mandić⁹³
L. Manhaes de Andrade Filho^{83a} I.M. Maniatis¹⁶⁹ J. Manjarres Ramos^{102,an} D.C. Mankad¹⁶⁹ A. Mann¹⁰⁹
B. Mansoulie¹³⁵ S. Manzoni³⁶ X. Mapekula^{33c} A. Marantis^{152,ac} G. Marchiori⁵ M. Marcisovsky¹³¹
C. Marcon^{71a,71b} M. Marinescu²⁰ M. Marjanovic¹²⁰ E.J. Marshall⁹¹ Z. Marshall^{17a} S. Marti-Garcia¹⁶³
T.A. Martin¹⁶⁷ V.J. Martin⁵² B. Martin dit Latour¹⁶ L. Martinelli^{75a,75b} M. Martinez^{13,ad}
P. Martinez Agullo¹⁶³ V.I. Martinez Outschoorn¹⁰³ P. Martinez Suarez¹³ S. Martin-Haugh¹³⁴
V.S. Martoiu^{27b} A.C. Martyniuk⁹⁶ A. Marzin³⁶ D. Mascione^{78a,78b} L. Masetti¹⁰⁰ T. Mashimo¹⁵³
J. Masik¹⁰¹ A.L. Maslennikov³⁷ L. Massa^{23b} P. Massarotti^{72a,72b} P. Mastrandrea^{74a,74b}
A. Mastroberardino^{43b,43a} T. Masubuchi¹⁵³ T. Mathisen¹⁶¹ J. Matousek¹³³ N. Matsuzawa¹⁵³ J. Maurer^{27b}
B. Maček⁹³ D.A. Maximov³⁷ R. Mazini¹⁴⁸ I. Maznas¹⁵² M. Mazza¹⁰⁷ S.M. Mazza¹³⁶
E. Mazzeo^{71a,71b} C. Mc Ginn²⁹ J.P. Mc Gowan¹⁰⁴ S.P. Mc Kee¹⁰⁶ E.F. McDonald¹⁰⁵
A.E. McDougall¹¹⁴ J.A. MCFayden¹⁴⁶ R.P. McGovern¹²⁸ G. Mchedlize^{149b} R.P. McKenzie^{33g}
T.C. McLachlan⁴⁸ D.J. McLaughlin⁹⁶ S.J. McMahon¹³⁴ C.M. Mcpartland⁹² R.A. McPherson^{165,ai}
S. Mehlhase¹⁰⁹ A. Mehta⁹² D. Melini¹⁵⁰ B.R. Mellado Garcia^{33g} A.H. Melo⁵⁵ F. Meloni⁴⁸
A.M. Mendes Jacques Da Costa¹⁰¹ H.Y. Meng¹⁵⁵ L. Meng⁹¹ S. Menke¹¹⁰ M. Mentink³⁶ E. Meoni^{43b,43a}
C. Merlassino¹²⁶ L. Merola^{72a,72b} C. Meroni^{71a,71b} G. Merz¹⁰⁶ O. Meshkov³⁷ J. Metcalfe⁶ A.S. Mete⁶
C. Meyer⁶⁸ J-P. Meyer¹³⁵ R.P. Middleton¹³⁴ L. Mijović⁵² G. Mikenberg¹⁶⁹ M. Mikestikova¹³¹
M. Mikuz⁹³ H. Mildner¹⁰⁰ A. Milic³⁶ C.D. Milke⁴⁴ D.W. Miller³⁹ L.S. Miller³⁴ A. Milov¹⁶⁹
D.A. Milstead^{47a,47b} T. Min^{14c} A.A. Minaenko³⁷ I.A. Minashvili^{149b} L. Mince⁵⁹ A.I. Mincer¹¹⁷
B. Mindur^{86a} M. Mineev³⁸ Y. Mino⁸⁸ L.M. Mir¹³ M. Miralles Lopez¹⁶³ M. Mironova^{17a}
A. Mishima¹⁵³ M.C. Missio¹¹³ A. Mitra¹⁶⁷ V.A. Mitsou¹⁶³ Y. Mitsumori¹¹¹ O. Miu¹⁵⁵
P.S. Miyagawa⁹⁴ T. Mkrtchyan^{63a} M. Mlinarevic⁹⁶ T. Mlinarevic⁹⁶ M. Mlynarikova³⁶ S. Mobius¹⁹
P. Moder⁴⁸ P. Mogg¹⁰⁹ A.F. Mohammed^{14a,14e} S. Mohapatra⁴¹ G. Mokgatitwane^{33g} L. Moleri¹⁶⁹
B. Mondal¹⁴¹ S. Mondal¹³² G. Monig¹⁴⁶ K. Mönig⁴⁸ E. Monnier¹⁰² L. Monsonis Romero¹⁶³
J. Montejo Berlingen¹³ M. Montella¹¹⁹ F. Montecelli^{77a,77b} F. Monticelli⁹⁰ S. Monzani^{69a,69c}
N. Morange⁶⁶ A.L. Moreira De Carvalho^{130a} M. Moreno Llácer¹⁶³ C. Moreno Martinez⁵⁶ P. Morettini^{57b}
S. Morgenstern³⁶ M. Morii⁶¹ M. Morinaga¹⁵³ A.K. Morley³⁶ F. Morodei^{75a,75b} L. Morvaj³⁶
P. Moschovakos³⁶ B. Moser³⁶ M. Mosidze^{149b} T. Moskalets⁵⁴ P. Moskvitina¹¹³ J. Moss^{31,p}

D. Pudza³⁷ D. Pyatiizbyantseva³⁷ J. Qian¹⁰⁶ R. Qian¹⁰⁷ D. Qichen¹⁰¹ Y. Qin¹⁰¹ T. Qiu⁵²
A. Quadt⁵⁵ M. Queitsch-Maitland¹⁰¹ G. Quetan⁵⁶ R.P. Quinn¹⁶⁴ G. Rabanal Bolanos⁶¹
D. Rafanoharana⁵⁴ F. Ragusa^{71a,71b} J.L. Rainbolt³⁹ J.A. Raine⁵⁶ S. Rajagopalan²⁹ E. Ramakoti³⁷
I.A. Ramirez-Berend¹³⁴ K. Ran^{48,14e} N.P. Rapheeha^{33g} H. Rasheed^{27b} V. Raskina¹²⁷ D.F. Rassloff^{63a}
S. Rave¹⁰⁰ B. Ravina⁵⁵ I. Ravinovich¹⁶⁹ M. Raymond¹³⁶ A.L. Read¹²⁵ N.P. Readloff¹³⁹
D.M. Rebuzzi^{73a,73b} G. Redlinger²⁹ A.S. Reed¹¹⁰ K. Reeves²⁶ J.A. Reidelsturz^{171,aa} D. Reikher¹⁵¹
A. Rej^{49,z} C. Rembser³⁶ A. Renardi⁴⁸ M. Renda^{27b} M.B. Rendel¹¹⁰ F. Renner⁴⁸ A.G. Rennie¹⁶⁰
A.L. Rescia⁴⁸ S. Resconi^{71a} M. Ressegotti^{57b,57a} S. Rettie³⁶ J.G. Reyes Rivera¹⁰⁷ E. Reynolds^{17a}
O.L. Rezanova³⁷ P. Reznicek¹³³ N. Ribaric⁹¹ E. Ricci^{78a,78b} R. Richter¹¹⁰ S. Richter^{47a,47b}
E. Richter-Was^{86b} M. Rideli¹²⁷ S. Ridouani^{35d} P. Rieck¹¹⁷ P. Riedler³⁶ E.M. Riefel^{147a,47b} J.O. Rieger¹¹⁴
M. Rijssenbeek¹⁴⁵ A. Rimoldi^{73a,73b} M. Rimoldi³⁶ L. Rinaldi^{23b,23a} T.T. Rinn²⁹ M.P. Rinnagel¹⁰⁹
G. Ripellino¹⁶¹ I. Riu¹³ P. Rivadeneira⁴⁸ J.C. Rivera Vergara¹⁶⁵ F. Rizatdinova¹²¹ E. Rizvi⁹⁴
B.A. Roberts¹⁶⁷ B.R. Roberts^{17a} S.H. Robertson^{104,ai} D. Robinson³² C.M. Robles Gajardo^{137f}
M. Robles Manzano¹⁰⁰ A. Robson⁵⁹ A. Rocchi^{76a,76b} C. Roda^{74a,74b} S. Rodriguez Bosca^{63a}
Y. Rodriguez Garcia^{22a} A. Rodriguez Rodriguez⁵⁴ A.M. Rodríguez Vera^{156b} S. Roe³⁶ J.T. Roemer¹⁶⁰
A.R. Roepe-Gier¹³⁶ J. Roggel¹⁷¹ O. Röhne¹²⁵ R.A. Rojas¹⁰³ C.P.A. Roland¹²⁷ J. Roloff²⁹
A. Romaniouk³⁷ E. Romano^{73a,73b} M. Romano^{23b} A.C. Romero Hernandez¹⁶² N. Rompotis⁹² L. Roos¹²⁷
S. Rosati^{75a} B.J. Rosser³⁹ E. Rossi¹²⁶ E. Rossi^{72a,72b} L.P. Rossi^{57b} L. Rossini⁵⁴ R. Rosten¹¹⁹
M. Rotaru^{27b} B. Rottler⁵⁴ C. Rougier^{102,an} D. Rousseau⁶⁶ D. Rouso³² A. Roy¹⁶² S. Roy-Garand¹⁵⁵
A. Rozanov¹⁰² Y. Rozen¹⁵⁰ X. Ruan^{33g} A. Rubio Jimenez¹⁶³ A.J. Ruby⁹² V.H. Ruelas Rivera¹⁸
T.A. Ruggieri¹ A. Ruggiero¹²⁶ A. Ruiz-Martinez¹⁶³ A. Rummler³⁶ Z. Rurikova⁵⁴ N.A. Rusakovich³⁸
H.L. Russell¹⁶⁵ G. Russo^{75a,75b} J.P. Rutherford⁷ S. Rutherford Colmenares³² K. Rybacki⁹¹ M. Rybar¹³³
E.B. Rye¹²⁵ A. Ryzhov⁴⁴ J.A. Sabater Iglesias⁵⁶ P. Sabatini¹⁶³ L. Sabetta^{75a,75b} H.F.W. Sadrozinski¹³⁶
F. Safai Tehrani^{75a} B. Safarzadeh Samani¹³⁴ M. Safdari¹⁴³ S. Saha¹⁶⁵ M. Sahinsoy¹¹⁰ M. Saimpert¹³⁵
M. Saito¹⁵³ T. Saito¹⁵³ D. Salamani³⁶ A. Salnikov¹⁴³ J. Salt¹⁶³ A. Salvador Salas¹⁵¹
D. Salvatore^{43b,43a} F. Salvatore¹⁴⁶ A. Salzburger³⁶ D. Sammel⁵⁴ D. Sampsonidis^{152,f} D. Sampsonidou¹²³
J. Sánchez¹⁶³ A. Sanchez Pineda⁴ V. Sanchez Sebastian¹⁶³ H. Sandaker¹²⁵ C.O. Sander⁴⁸
J.A. Sandesara¹⁰³ M. Sandhoff¹⁷¹ C. Sandoval^{22b} D.P.C. Sankey¹³⁴ T. Sano⁸⁸ A. Sansoni⁵³
L. Santi^{75a,75b} C. Santoni⁴⁰ H. Santos^{130a,130b} S.N. Santpur^{17a} A. Santra¹⁶⁹ K.A. Saoucha^{116b}
J.G. Saraiva^{130a,130d} J. Sardain⁷ O. Sasaki⁸⁴ K. Sato¹⁵⁷ C. Sauer^{63b} F. Sauerburger⁵⁴ E. Sauvan⁴
P. Savard^{155,aw} R. Sawada¹⁵³ C. Sawyer¹³⁴ L. Sawyer⁹⁷ I. Sayago Galvan¹⁶³ C. Sbarra^{23b}
A. Sbrizzi^{23b,23a} T. Scanlon⁹⁶ J. Schaarschmidt¹³⁸ P. Schacht¹¹⁰ U. Schäfer¹⁰⁰ A.C. Schaffer^{66,44}
D. Schaile¹⁰⁹ R.D. Schamberger¹⁴⁵ C. Scharf⁴⁸ M.M. Schefer¹⁹ V.A. Schegelsky³⁷ D. Scheirich¹³³
F. Schenck¹⁸ M. Schernau¹⁶⁰ C. Scheulen⁵⁵ C. Schiavi^{57b,57a} E.J. Schioppa^{70a,70b} M. Schioppa^{43b,43a}
B. Schlag^{143,i} K.E. Schleicher⁵⁴ S. Schlenker³⁶ J. Schmeing¹⁷¹ M.A. Schmidt¹⁷¹ K. Schmieden¹⁰⁰
C. Schmitt¹⁰⁰ N. Schmitt¹⁰⁰ S. Schmitt⁴⁸ L. Schoeffel¹³⁵ A. Schoening^{63b} P.G. Scholer⁵⁴
E. Schopf¹²⁶ M. Schott¹⁰⁰ J. Schovancova³⁶ S. Schramm⁵⁶ F. Schroeder¹⁷¹ T. Schroer⁵⁶
H-C. Schultz-Coulon^{63a} M. Schumacher⁵⁴ B.A. Schumm¹³⁶ Ph. Schune¹³⁵ A.J. Schuy¹³⁸
H.R. Schwartz¹³⁶ A. Schwartzman¹⁴³ T.A. Schwarz¹⁰⁶ Ph. Schwemling¹³⁵ R. Schwienhorst¹⁰⁷
A. Sciandra¹³⁶ G. Sciolla²⁶ F. Scuri^{74a} C.D. Sebastiani⁹² K. Sedlaczek¹¹⁵ P. Seema¹⁸ S.C. Seidel¹¹²
A. Seiden¹³⁶ B.D. Seidlitz⁴¹ C. Seitz⁴⁸ J.M. Seixas^{83b} G. Sekhniaidze^{72a} S.J. Sekula⁴⁴ L. Selim⁶⁰
N. Semprini-Cesari^{23b,23a} D. Sengupta⁵⁶ V. Senthilkumar¹⁶³ L. Serin⁶⁶ L. Serkin^{69a,69b} M. Sessa^{76a,76b}
H. Severini¹²⁰ F. Sforza^{57b,57a} A. Sfyrla⁵⁶ E. Shabalina⁵⁵ R. Shaheen¹⁴⁴ J.D. Shahinian¹²⁸
D. Shaked Renous¹⁶⁹ L.Y. Shan^{14a} M. Shapiro^{17a} A. Sharma³⁶ A.S. Sharma¹⁶⁴ P. Sharma⁸⁰
S. Sharma⁴⁸ P.B. Shatalov³⁷ K. Shaw¹⁴⁶ S.M. Shaw¹⁰¹ A. Shcherbakova³⁷ Q. Shen^{62c,5}
P. Sherwood⁹⁶ L. Shi⁹⁶ X. Shi^{14a} C.O. Shimmin¹⁷² J.D. Shinner⁹⁵ I.P.J. Shipsey¹²⁶ S. Shirabe^{56j}

M. Shiyakova^{38,ag} J. Shlomi¹⁶⁹ M.J. Shochet³⁹ J. Shojaii¹⁰⁵ D.R. Shope¹²⁵ B. Shrestha¹²⁰
 S. Shrestha^{119,ba} E.M. Shrif^{43g} M.J. Shroff¹⁶⁵ P. Sicho¹³¹ A.M. Sickles¹⁶² E. Sideras Haddad^{133g}
 A. Sidoti^{23b} F. Siegert⁵⁰ Dj. Sijacki¹⁵ R. Sikora^{86a} F. Sili⁹⁰ J.M. Silva²⁰ M.V. Silva Oliveira²⁹
 S.B. Silverstein^{47a} S. Simion⁶⁶ R. Simoniello³⁶ E.L. Simpson⁵⁹ H. Simpson¹⁴⁶ L.R. Simpson¹⁰⁶
 N.D. Simpson⁹⁸ S. Simsek⁸² S. Sindhu⁵⁵ P. Sinervo¹⁵⁵ S. Singh¹⁵⁵ S. Sinha⁴⁸ S. Sinha¹⁰¹
 M. Sioli^{23b,23a} I. Siral³⁶ E. Sitnikova⁴⁸ S.Yu. Sivoklokov^{37,*} J. Sjölin^{47a,47b} A. Skaf⁵⁵ E. Skorda^{20,ar}
 P. Skubic¹²⁰ M. Slawinska⁸⁷ V. Smakhtin¹⁶⁹ B.H. Smart¹³⁴ J. Smiesko³⁶ S.Yu. Smirnov³⁷
 Y. Smirnov³⁷ L.N. Smirnova^{37,a} O. Smirnova⁹⁸ A.C. Smith⁴¹ E.A. Smith³⁹ H.A. Smith¹²⁶
 J.L. Smith⁹² R. Smith¹⁴³ M. Smizanska⁹¹ K. Smolek¹³² A.A. Snesarev³⁷ S.R. Snider¹⁵⁵ H.L. Snoek¹¹⁴
 S. Snyder²⁹ R. Sobie^{165,ai} A. Soffer¹⁵¹ C.A. Solans Sanchez³⁶ E.Yu. Soldatov³⁷ U. Soldevila¹⁶³
 A.A. Solodkov³⁷ S. Solomon²⁶ A. Soloshenko³⁸ K. Solovieva⁵⁴ O.V. Solovyanov⁴⁰ V. Solovyev³⁷
 P. Sommer³⁶ A. Sonay¹³ W.Y. Song^{156b} J.M. Sonneveld¹¹⁴ A. Sopczak¹³² A.L. Sopic⁹⁶
 F. Sopkova^{28b} I.R. Sotarriva Alvarez¹⁵⁴ V. Sothilingam^{63a} S. Sottocornola⁶⁸ R. Soualah^{116b}
 Z. Soumami^{35e} D. South⁴⁸ N. Soybelman¹⁶⁹ S. Spagnolo^{70a,70b} M. Spalla¹¹⁰ D. Sperlich⁵⁴
 G. Spigo³⁶ S. Spinali⁹¹ D.P. Spiteri⁵⁹ M. Spousta¹³³ E.J. Staats³⁴ A. Stabile^{71a,71b} R. Stamen^{63a}
 A. Stampekis²⁰ M. Standke²⁴ E. Stanecka⁸⁷ M.V. Stange⁵⁰ B. Stanislaus^{17a} M.M. Stanitzki⁴⁸
 B. Stapi⁴⁸ E.A. Starchenko³⁷ G.H. Stark¹³⁶ J. Stark^{102,an} D.M. Starke^{156b} P. Staroba¹³¹
 P. Starovoitov^{63a} S. Stärz¹⁰⁴ R. Staszewski⁸⁷ G. Stavropoulos⁴⁶ J. Steentoft¹⁶¹ P. Steinberg²⁹
 B. Stelzer^{142,156a} H.J. Stelzer¹²⁹ O. Stelzer-Chilton^{156a} H. Stenzel¹⁵⁸ T.J. Stevenson¹⁴⁶ G.A. Stewart³⁶
 J.R. Stewart¹²¹ M.C. Stockton³⁶ G. Stoicea^{27b} M. Stolarski^{130a} S. Stonjek¹¹⁰ A. Straessner⁵⁰
 J. Strandberg¹⁴⁴ S. Strandberg^{47a,47b} M. Stratmann¹⁷¹ M. Strauss¹²⁰ T. Streblner¹⁰² P. Strizenc^{28b}
 R. Ströhmer¹⁶⁶ D.M. Strom¹²³ L.R. Strom⁴⁸ R. Stroynowski⁴⁴ A. Strubig^{47a,47b} S.A. Stucci²⁹
 B. Stugu¹⁶ J. Stupak¹²⁰ N.A. Styles⁴⁸ D. Su¹⁴³ S. Su^{62a} W. Su^{62d} X. Su^{62a,66} K. Sugizaki¹⁵³
 V.V. Sulim³⁷ M.J. Sullivan⁹² D.M.S. Sultan^{78a,78b} L. Sultanaliev³⁷ S. Sultansoy^{3b} T. Sumida⁸⁸
 S. Sun¹⁰⁶ S. Sun¹⁷⁰ O. Sunneborn Gudnadottir¹⁶¹ N. Sur¹⁰² M.R. Sutton¹⁴⁶ H. Suzuki¹⁵⁷
 M. Svatos¹³¹ M. Swiatlowski^{156a} T. Swirski¹⁶⁶ I. Sykora^{28a} M. Sykora¹³³ T. Sykora¹³³ D. Ta¹⁰⁰
 K. Tackmann^{48,ac} A. Taffard¹⁶⁰ R. Tafirout^{156a} J.S. Tafuya Vargas⁶⁶ E.P. Takeva⁵² Y. Takubo⁸⁴
 M. Talby¹⁰² A.A. Talyshev³⁷ K.C. Tam^{64b} N.M. Tamir¹⁵¹ A. Tanaka¹⁵³ J. Tanaka¹⁵³ R. Tanaka⁶⁶
 M. Tanasini^{57b,57a} Z. Tao¹⁶⁴ S. Tapia Araya^{137f} S. Tapprogge¹⁰⁰ A. Tarek Abouelfadl Mohamed¹⁰⁷
 S. Tarem¹⁵⁰ K. Tariq^{14a} G. Tarna^{102,27b} G.F. Tartarelli^{71a} P. Tas¹³³ M. Tasevsky¹³¹ E. Tassi^{43b,43a}
 A.C. Tate¹⁶² G. Tateno¹⁵³ Y. Tayalati^{35e,ah} G.N. Taylor¹⁰⁵ W. Taylor^{156b} A.S. Tee¹⁷⁰
 R. Teixeira De Lima¹⁴³ P. Teixeira-Dias⁹⁵ J.J. Teoh¹⁵⁵ K. Terashi¹⁵³ J. Terron⁹⁹ S. Terzo¹³
 M. Testa⁵³ R.J. Teuscher^{155,ai} A. Thaler⁷⁹ O. Theiner⁵⁶ N. Themistokleous⁵² T. Theveneaux-Pelzer¹⁰²
 O. Thielmann¹⁷¹ D.W. Thomas⁹⁵ J.P. Thomas²⁰ E.A. Thompson^{17a} P.D. Thompson²⁰ E. Thomson¹²⁸
 Y. Tian⁵⁵ V. Tikhomirov^{37,a} Yu.A. Tikhonov³⁷ S. Timoshenko³⁷ D. Timoshyn¹³³ E.X.L. Ting¹
 P. Tipton¹⁷² S.H. Tlou^{33g} A. Tmourji⁴⁰ K. Todome¹⁵⁴ S. Todorova-Nova¹³³ S. Todt⁵⁰ M. Togawa⁸⁴
 J. Tojo⁸⁹ S. Tokár^{28a} K. Tokushuku⁸⁴ O. Toldaiev⁶⁸ R. Tombs³² M. Tomoto^{84,111} L. Tompkins^{143,t}
 K.W. Topolnicki^{86b} E. Torrence¹²³ H. Torres^{102,an} E. Torró Pastor¹⁶³ M. Toscani³⁰ C. Toscirri³⁹
 M. Tost¹¹ D.R. Tovey¹³⁹ A. Traeet¹⁶ I.S. Trandafir^{27b} T. Trefzger¹⁶⁶ A. Tricoli²⁹ I.M. Trigger^{156a}
 S. Trincz-Duvoid¹²⁷ D.A. Trischuk²⁶ B. Trocme⁶⁰ C. Troncon^{71a} L. Truong^{33c} M. Trzebinski⁸⁷
 A. Trzupek⁸⁷ F. Tsai¹⁴⁵ M. Tsai¹⁰⁶ A. Tsiamis^{152,f} P.V. Tsiarashka³⁷ S. Tsigaridas^{156a}
 A. Tsigotis^{152,ac} V. Tsiskaridze¹⁵⁵ E.G. Tskhadadze^{149a} M. Tsopoulou^{152,f} Y. Tsujikawa⁸⁸
 I.I. Tsukerman³⁷ V. Tsulaia^{17a} S. Tsuno⁸⁴ O. Tsur¹⁵⁰ K. Tsurii¹¹⁸ D. Tsybychev¹⁴⁵ Y. Tu^{64b}
 A. Tudorache^{27b} V. Tudorache^{27b} A.N. Tuna³⁶ S. Turchikhin^{57b,57a} I. Turk Cakir^{3a} R. Turra^{71a}
 T. Turtuvshin^{38,aj} P.M. Tuts⁴¹ S. Tzamarias^{152,f} P. Tzani¹⁰ E. Tzovara¹⁰⁰ F. Ukegawa¹⁵⁷
 P.A. Ulloa Poblete^{137c,137b} E.N. Umaka²⁹ G. Unal³⁶ M. Unal¹¹ A. Undrus²⁹ G. Unel¹⁶⁰ J. Urban^{28b}

Y. Zhang^{14c}  Z. Zhang^{17a}  Z. Zhang⁶⁶  H. Zhao¹³⁸  P. Zhao⁵¹  T. Zhao^{62b}  Y. Zhao¹³⁶  Z. Zhao^{62a} 
 A. Zhemchugov³⁸  J. Zheng^{14c}  K. Zheng¹⁶²  X. Zheng^{62a}  Z. Zheng¹⁴³  D. Zhong¹⁶²  B. Zhou¹⁰⁶
 H. Zhou⁷  N. Zhou^{62c}  Y. Zhou⁷ C.G. Zhu^{62b}  J. Zhu¹⁰⁶  Y. Zhu^{62c}  Y. Zhu^{62a}  X. Zhuang^{14a} 
 K. Zhukov³⁷  V. Zhulanov³⁷  N.I. Zimine³⁸  J. Zinsser^{63b}  M. Ziolkowski¹⁴¹  L. Živković¹⁵ 
 A. Zoccoli^{23b,23a}  K. Zoch⁶¹  T.G. Zorbas¹³⁹  O. Zormpa⁴⁶  W. Zou⁴¹  L. Zwalinski³⁶ 

¹Department of Physics, University of Adelaide, Adelaide, Australia

²Department of Physics, University of Alberta, Edmonton AB, Canada

^{3a}Department of Physics, Ankara University, Ankara, Türkiye

^{3b}Division of Physics, TOBB University of Economics and Technology, Ankara, Türkiye

⁴LAPP, Université Savoie Mont Blanc, CNRS/IN2P3, Annecy, France

⁵APC, Université Paris Cité, CNRS/IN2P3, Paris, France

⁶High Energy Physics Division, Argonne National Laboratory, Argonne IL, United States of America

⁷Department of Physics, University of Arizona, Tucson AZ, United States of America

⁸Department of Physics, University of Texas at Arlington, Arlington TX, United States of America

⁹Physics Department, National and Kapodistrian University of Athens, Athens, Greece

¹⁰Physics Department, National Technical University of Athens, Zografou, Greece

¹¹Department of Physics, University of Texas at Austin, Austin TX, United States of America

¹²Institute of Physics, Azerbaijan Academy of Sciences, Baku, Azerbaijan

¹³Institut de Física d'Altes Energies (IFAE), Barcelona Institute of Science and Technology, Barcelona, Spain

^{14a}Institute of High Energy Physics, Chinese Academy of Sciences, Beijing

^{14b}Physics Department, Tsinghua University, Beijing

^{14c}Department of Physics, Nanjing University, Nanjing

^{14d}School of Science, Shenzhen Campus of Sun Yat-sen University, Shenzhen

^{14e}University of Chinese Academy of Science (UCAS), Beijing

¹⁵Institute of Physics, University of Belgrade, Belgrade, Serbia

¹⁶Department for Physics and Technology, University of Bergen, Bergen, Norway

^{17a}Physics Division, Lawrence Berkeley National Laboratory, Berkeley CA, United States of America

^{17b}University of California, Berkeley CA, United States of America

¹⁸Institut für Physik, Humboldt Universität zu Berlin, Berlin, Germany

¹⁹Albert Einstein Center for Fundamental Physics and Laboratory for High Energy Physics, University of Bern, Bern, Switzerland

²⁰School of Physics and Astronomy, University of Birmingham, Birmingham, United Kingdom

^{21a}Department of Physics, Bogazici University, Istanbul, Türkiye

^{21b}Department of Physics Engineering, Gaziantep University, Gaziantep, Türkiye

^{21c}Department of Physics, Istanbul University, Istanbul, Türkiye

^{22a}Facultad de Ciencias y Centro de Investigaciones, Universidad Antonio Nariño, Bogotá, Colombia

^{22b}Departamento de Física, Universidad Nacional de Colombia, Bogotá, Colombia

^{23a}Dipartimento di Fisica e Astronomia A. Righi, Università di Bologna, Bologna, Italy

^{23b}INFN Sezione di Bologna, Italy

²⁴Physikalisches Institut, Universität Bonn, Bonn, Germany

²⁵Department of Physics, Boston University, Boston MA, United States of America

²⁶Department of Physics, Brandeis University, Waltham MA, United States of America

^{27a}Transilvania University of Brasov, Brasov, Romania

^{27b}Horia Hulubei National Institute of Physics and Nuclear Engineering, Bucharest, Romania

^{27c}Department of Physics, Alexandru Ioan Cuza University of Iasi, Iasi, Romania

^{27d}National Institute for Research and Development of Isotopic and Molecular Technologies, Physics Department, Cluj-Napoca, Romania

^{27e}University Politehnica Bucharest, Bucharest, Romania

^{27f}West University in Timisoara, Timisoara, Romania

^{27g}Faculty of Physics, University of Bucharest, Bucharest, Romania

^{28a}Faculty of Mathematics, Physics and Informatics, Comenius University, Bratislava, Slovak Republic

^{28b}Department of Subnuclear Physics, Institute of Experimental Physics of the Slovak Academy of Sciences, Kosice, Slovak Republic

²⁹Physics Department, Brookhaven National Laboratory, Upton NY, United States of America

³⁰Universidad de Buenos Aires, Facultad de Ciencias Exactas y Naturales, Departamento de Física, y CONICET, Instituto de Física de Buenos Aires (IFIBA), Buenos Aires, Argentina

³¹California State University, CA, United States of America

³²Cavendish Laboratory, University of Cambridge, Cambridge, United Kingdom

^{33a}Department of Physics, University of Cape Town, Cape Town, South Africa

^{33b}Themba Labs, Western Cape, South Africa

^{33c}Department of Mechanical Engineering Science, University of Johannesburg, Johannesburg, South Africa

^{33d}National Institute of Physics, University of the Philippines Diliman (Philippines), South Africa

^{33e}University of South Africa, Department of Physics, Pretoria, South Africa

^{33f}University of Zululand, KwaDlangezwa, South Africa

^{33g}School of Physics, University of the Witwatersrand, Johannesburg, South Africa

³⁴Department of Physics, Carleton University, Ottawa ON, Canada

^{35a}Faculté des Sciences Ain Chock, Réseau Universitaire de Physique des Hautes Energies - Université Hassan II, Casablanca, Morocco

^{35b}Faculté des Sciences, Université Ibn-Tofail, Kénitra, Morocco

^{35c}Faculté des Sciences Semlalia, Université Cadi Ayyad, LPHEA-Marrakech, Morocco

- ^{35d}LPMR, Faculté des Sciences, Université Mohamed Premier, Oujda, Morocco
^{35e}Faculté des sciences, Université Mohammed V, Rabat, Morocco
^{35f}Institute of Applied Physics, Mohammed VI Polytechnic University, Ben Guerir, Morocco
³⁶CERN, Geneva, Switzerland
³⁷Affiliated with an institute covered by a cooperation agreement with CERN
³⁸Affiliated with an international laboratory covered by a cooperation agreement with CERN
³⁹Enrico Fermi Institute, University of Chicago, Chicago IL, United States of America
⁴⁰LPC, Université Clermont Auvergne, CNRS/IN2P3, Clermont-Ferrand, France
⁴¹Nevis Laboratory, Columbia University, Irvington NY, United States of America
⁴²Niels Bohr Institute, University of Copenhagen, Copenhagen, Denmark
^{43a}Dipartimento di Fisica, Università della Calabria, Rende, Italy
^{43b}INFN Gruppo Collegato di Cosenza, Laboratori Nazionali di Frascati, Italy
⁴⁴Physics Department, Southern Methodist University, Dallas TX, United States of America
⁴⁵Physics Department, University of Texas at Dallas, Richardson TX, United States of America
⁴⁶National Centre for Scientific Research "Demokritos", Agia Paraskevi, Greece
^{47a}Department of Physics, Stockholm University, Sweden
^{47b}Oskar Klein Centre, Stockholm, Sweden
⁴⁸Deutsches Elektronen-Synchrotron DESY, Hamburg and Zeuthen, Germany
⁴⁹Fakultät Physik, Technische Universität Dortmund, Dortmund, Germany
⁵⁰Institut für Kern- und Teilchenphysik, Technische Universität Dresden, Dresden, Germany
⁵¹Department of Physics, Duke University, Durham NC, United States of America
⁵²SUPA - School of Physics and Astronomy, University of Edinburgh, Edinburgh, United Kingdom
⁵³INFN e Laboratori Nazionali di Frascati, Frascati, Italy
⁵⁴Physikalisches Institut, Albert-Ludwigs-Universität Freiburg, Freiburg, Germany
⁵⁵II. Physikalisches Institut, Georg-August-Universität Göttingen, Göttingen, Germany
⁵⁶Département de Physique Nucléaire et Corpusculaire, Université de Genève, Genève, Switzerland
^{57a}Dipartimento di Fisica, Università di Genova, Genova, Italy
^{57b}INFN Sezione di Genova, Italy
⁵⁸II. Physikalisches Institut, Justus-Liebig-Universität Giessen, Giessen, Germany
⁵⁹SUPA - School of Physics and Astronomy, University of Glasgow, Glasgow, United Kingdom
⁶⁰LPC, Université Grenoble Alpes, CNRS/IN2P3, Grenoble INP, Grenoble, France
⁶¹Laboratory for Particle Physics and Cosmology, Harvard University, Cambridge MA, United States of America
^{62a}Department of Modern Physics and State Key Laboratory of Particle Detection and Electronics, University of Science and Technology of China, Hefei
^{62b}Institute of Frontier and Interdisciplinary Science and Key Laboratory of Particle Physics and Particle Irradiation (MOE), Shandong University, Qingdao
^{62c}School of Physics and Astronomy, Shanghai Jiao Tong University, Key Laboratory for Particle Astrophysics and Cosmology (MOE), SKLPPC, Shanghai
^{62d}Tsung-Dao Lee Institute, Shanghai
^{63a}Kirchhoff-Institut für Physik, Ruprecht-Karls-Universität Heidelberg, Heidelberg, Germany
^{63b}Physikalisches Institut, Ruprecht-Karls-Universität Heidelberg, Heidelberg, Germany
^{64a}Department of Physics, Chinese University of Hong Kong, Shatin, N.T., Hong Kong
^{64b}Department of Physics, University of Hong Kong, Hong Kong
^{64c}Department of Physics and Institute for Advanced Study, Hong Kong, China University of Science and Technology, Clear Water Bay, Kowloon, Hong Kong
⁶⁵Department of Physics, National Tsing Hua University, Hsinchu
⁶⁶IJCLab, Université Paris-Saclay, CNRS/IN2P3, 91405, Orsay, France
⁶⁷Centro Nacional de Microelectrónica (IMB-CNM-CSIC), Barcelona, Spain
⁶⁸Department of Physics, Indiana University, Bloomington IN, United States of America
^{69a}INFN Gruppo Collegato di Udine, Sezione di Trieste, Udine, Italy
^{69b}ICTP, Trieste, Italy
^{69c}Dipartimento Politecnico di Ingegneria e Architettura, Università di Udine, Udine, Italy
^{70a}INFN Sezione di Lecce, Italy
^{70b}Dipartimento di Matematica e Fisica, Università del Salento, Lecce, Italy
^{71a}INFN Sezione di Milano, Italy
^{71b}Dipartimento di Fisica, Università di Milano, Milano, Italy
^{72a}INFN Sezione di Napoli, Italy
^{72b}Dipartimento di Fisica, Università di Napoli, Napoli, Italy
^{73a}INFN Sezione di Pavia, Italy
^{73b}Dipartimento di Fisica, Università di Pavia, Pavia, Italy
^{74a}INFN Sezione di Pisa, Italy
^{74b}Dipartimento di Fisica E. Fermi, Università di Pisa, Pisa, Italy
^{75a}INFN Sezione di Roma, Italy
^{75b}Dipartimento di Fisica, Sapienza Università di Roma, Roma, Italy
^{76a}INFN Sezione di Roma Tor Vergata
^{76b}Dipartimento di Fisica, Università di Roma Tor Vergata, Roma, Italy
^{77a}INFN Sezione di Roma Tre, Italy
^{77b}Dipartimento di Matematica e Fisica, Università Roma Tre, Roma, Italy

- ^{78a}INFN-TIFPA, Italy
^{78b}Università degli Studi di Trento, Trento, Italy
⁷⁹Universität Innsbruck, Department of Astro and Particle Physics, Innsbruck, Austria
⁸⁰University of Iowa, Iowa City IA, United States of America
⁸¹Department of Physics and Astronomy, Iowa State University, Ames IA, United States of America
⁸²Istinye University, Sariyer, Istanbul, Türkiye
^{83a}Departamento de Engenharia Elétrica, Universidade Federal de Juiz de Fora (UFJF), Juiz de Fora, Brazil
^{83b}Universidade Federal do Rio De Janeiro COPPE/EE/IF, Rio de Janeiro, Brazil
^{83c}Instituto de Física, Universidade de São Paulo, São Paulo, Brazil
^{83d}Rio de Janeiro State University, Rio de Janeiro, Brazil
⁸⁴KEK, High Energy Accelerator Research Organization, Tsukuba, Japan
⁸⁵Graduate School of Science, Kobe University, Kobe, Japan
^{86a}AGH University of Krakow, Faculty of Physics and Applied Computer Science, Krakow, Poland
^{86b}Marian Smoluchowski Institute of Physics, Jagiellonian University, Krakow, Poland
⁸⁷Institute of Nuclear Physics Polish Academy of Sciences, Krakow, Poland
⁸⁸Faculty of Science, Kyoto University, Kyoto, Japan
⁸⁹Research Center for Advanced Particle Physics and Department of Physics, Kyushu University, Fukuoka, Japan
⁹⁰Instituto de Física La Plata, Universidad Nacional de La Plata and CONICET, La Plata, Argentina
⁹¹Physics Department, Lancaster University, Lancaster, United Kingdom
⁹²Oliver Lodge Laboratory, University of Liverpool, Liverpool, United Kingdom
⁹³Department of Experimental Particle Physics, Jožef Stefan Institute and Department of Physics, University of Ljubljana, Ljubljana, Slovenia
⁹⁴School of Physics and Astronomy, Queen Mary University of London, London, United Kingdom
⁹⁵Department of Physics, Royal Holloway University of London, Egham, United Kingdom
⁹⁶Department of Physics and Astronomy, University College London, London, United Kingdom
⁹⁷Louisiana Tech University, Ruston LA, United States of America
⁹⁸Fysiska institutionen, Lunds universitet, Lund, Sweden
⁹⁹Departamento de Física Teórica C-15 and CIAFF, Universidad Autónoma de Madrid, Madrid, Spain
¹⁰⁰Institut für Physik, Universität Mainz, Mainz, Germany
¹⁰¹School of Physics and Astronomy, University of Manchester, Manchester, United Kingdom
¹⁰²CPPM, Aix-Marseille Université, CNRS/IN2P3, Marseille, France
¹⁰³Department of Physics, University of Massachusetts, Amherst MA, United States of America
¹⁰⁴Department of Physics, McGill University, Montreal QC, Canada
¹⁰⁵School of Physics, University of Melbourne, Victoria, Australia
¹⁰⁶Department of Physics, University of Michigan, Ann Arbor MI, United States of America
¹⁰⁷Department of Physics and Astronomy, Michigan State University, East Lansing MI, United States of America
¹⁰⁸Group of Particle Physics, University of Montreal, Montreal QC, Canada
¹⁰⁹Fakultät für Physik, Ludwig-Maximilians-Universität München, München, Germany
¹¹⁰Max-Planck-Institut für Physik (Werner-Heisenberg-Institut), München, Germany
¹¹¹Graduate School of Science and Kobayashi-Maskawa Institute, Nagoya University, Nagoya, Japan
¹¹²Department of Physics and Astronomy, University of New Mexico, Albuquerque NM, United States of America
¹¹³Institute for Mathematics, Astrophysics and Particle Physics, Radboud University/Nikhef, Nijmegen, Netherlands
¹¹⁴Nikhef National Institute for Subatomic Physics and University of Amsterdam, Amsterdam, Netherlands
¹¹⁵Department of Physics, Northern Illinois University, DeKalb IL, United States of America
^{116a}New York University Abu Dhabi, Abu Dhabi, United Arab Emirates
^{116b}University of Sharjah, Sharjah, United Arab Emirates
¹¹⁷Department of Physics, New York University, New York NY, United States of America
¹¹⁸Ochanomizu University, Otsuka, Bunkyo-ku, Tokyo, Japan
¹¹⁹Ohio State University, Columbus OH, United States of America
¹²⁰Homer L. Dodge Department of Physics and Astronomy, University of Oklahoma, Norman OK, United States of America
¹²¹Department of Physics, Oklahoma State University, Stillwater OK, United States of America
¹²²Palacký University, Joint Laboratory of Optics, Olomouc, Czech Republic
¹²³Institute for Fundamental Science, University of Oregon, Eugene, OR, United States of America
¹²⁴Graduate School of Science, Osaka University, Osaka, Japan
¹²⁵Department of Physics, University of Oslo, Oslo, Norway
¹²⁶Department of Physics, Oxford University, Oxford, United Kingdom
¹²⁷LPNHE, Sorbonne Université, Université Paris Cité, CNRS/IN2P3, Paris, France
¹²⁸Department of Physics, University of Pennsylvania, Philadelphia PA, United States of America
¹²⁹Department of Physics and Astronomy, University of Pittsburgh, Pittsburgh PA, United States of America
^{130a}Laboratório de Instrumentação e Física Experimental de Partículas - LIP, Lisboa, Portugal
^{130b}Departamento de Física, Faculdade de Ciências, Universidade de Lisboa, Lisboa, Portugal
^{130c}Departamento de Física, Universidade de Coimbra, Coimbra, Portugal
^{130d}Centro de Física Nuclear da Universidade de Lisboa, Lisboa, Portugal
^{130e}Departamento de Física, Universidade do Minho, Braga, Portugal
^{130f}Departamento de Física Teórica y del Cosmos, Universidad de Granada, Granada (Spain), Portugal
^{130g}Departamento de Física, Instituto Superior Técnico, Universidade de Lisboa, Lisboa, Portugal
¹³¹Institute of Physics of the Czech Academy of Sciences, Prague, Czech Republic
¹³²Czech Technical University in Prague, Prague, Czech Republic
¹³³Charles University, Faculty of Mathematics and Physics, Prague, Czech Republic

- ¹³⁴Particle Physics Department, Rutherford Appleton Laboratory, Didcot, United Kingdom
- ¹³⁵IRFU, CEA, Université Paris-Saclay, Gif-sur-Yvette, France
- ¹³⁶Santa Cruz Institute for Particle Physics, University of California Santa Cruz, Santa Cruz CA, United States of America
- ^{137a}Departamento de Física, Pontificia Universidad Católica de Chile, Santiago, Chile
- ^{137b}Millennium Institute for Subatomic physics at high energy frontier (SAPHIR), Santiago, Chile
- ^{137c}Instituto de Investigación Multidisciplinario en Ciencia y Tecnología, y Departamento de Física, Universidad de La Serena, Chile
- ^{137d}Universidad Andres Bello, Department of Physics, Santiago, Chile
- ^{137e}Instituto de Alta Investigación, Universidad de Tarapacá, Arica, Chile
- ^{137f}Departamento de Física, Universidad Técnica Federico Santa María, Valparaíso, Chile
- ¹³⁸Department of Physics, University of Washington, Seattle WA, United States of America
- ¹³⁹Department of Physics and Astronomy, University of Sheffield, Sheffield, United Kingdom
- ¹⁴⁰Department of Physics, Shinshu University, Nagano, Japan
- ¹⁴¹Department Physik, Universität Siegen, Siegen, Germany
- ¹⁴²Department of Physics, Simon Fraser University, Burnaby BC, Canada
- ¹⁴³SLAC National Accelerator Laboratory, Stanford CA, United States of America
- ¹⁴⁴Department of Physics, Royal Institute of Technology, Stockholm, Sweden
- ¹⁴⁵Departments of Physics and Astronomy, Stony Brook University, Stony Brook NY, United States of America
- ¹⁴⁶Department of Physics and Astronomy, University of Sussex, Brighton, United Kingdom
- ¹⁴⁷School of Physics, University of Sydney, Sydney, Australia
- ¹⁴⁸Institute of Physics, Academia Sinica, Taipei
- ^{149a}E. Andronikashvili Institute of Physics, Iv. Javakishvili Tbilisi State University, Tbilisi, Georgia
- ^{149b}High Energy Physics Institute, Tbilisi State University, Tbilisi, Georgia
- ^{149c}University of Georgia, Tbilisi, Georgia
- ¹⁵⁰Department of Physics, Technion, Israel Institute of Technology, Haifa, Israel
- ¹⁵¹Raymond and Beverly Sackler School of Physics and Astronomy, Tel Aviv University, Tel Aviv, Israel
- ¹⁵²Department of Physics, Aristotle University of Thessaloniki, Thessaloniki, Greece
- ¹⁵³International Center for Elementary Particle Physics and Department of Physics, University of Tokyo, Tokyo, Japan
- ¹⁵⁴Department of Physics, Tokyo Institute of Technology, Tokyo, Japan
- ¹⁵⁵Department of Physics, University of Toronto, Toronto ON, Canada
- ^{156a}TRIUMF, Vancouver BC, Canada
- ^{156b}Department of Physics and Astronomy, York University, Toronto ON, Canada
- ¹⁵⁷Division of Physics and Tomonaga Center for the History of the Universe, Faculty of Pure and Applied Sciences, University of Tsukuba, Tsukuba, Japan
- ¹⁵⁸Department of Physics and Astronomy, Tufts University, Medford MA, United States of America
- ¹⁵⁹United Arab Emirates University, Al Ain, United Arab Emirates
- ¹⁶⁰Department of Physics and Astronomy, University of California Irvine, Irvine CA, United States of America
- ¹⁶¹Department of Physics and Astronomy, University of Uppsala, Uppsala, Sweden
- ¹⁶²Department of Physics, University of Illinois, Urbana IL, United States of America
- ¹⁶³Instituto de Física Corpuscular (IFIC), Centro Mixto Universidad de Valencia - CSIC, Valencia, Spain
- ¹⁶⁴Department of Physics, University of British Columbia, Vancouver BC, Canada
- ¹⁶⁵Department of Physics and Astronomy, University of Victoria, Victoria BC, Canada
- ¹⁶⁶Fakultät für Physik und Astronomie, Julius-Maximilians-Universität Würzburg, Würzburg, Germany
- ¹⁶⁷Department of Physics, University of Warwick, Coventry, United Kingdom
- ¹⁶⁸Waseda University, Tokyo, Japan
- ¹⁶⁹Department of Particle Physics and Astrophysics, Weizmann Institute of Science, Rehovot, Israel
- ¹⁷⁰Department of Physics, University of Wisconsin, Madison WI, United States of America
- ¹⁷¹Fakultät für Mathematik und Naturwissenschaften, Fachgruppe Physik, Bergische Universität Wuppertal, Wuppertal, Germany
- ¹⁷²Department of Physics, Yale University, New Haven CT, United States of America
- ^aAlso Affiliated with an institute covered by a cooperation agreement with CERN
- ^bAlso at An-Najah National University, Nablus, Palestine
- ^cAlso at APC, Université Paris Cité, CNRS/IN2P3, Paris, France
- ^dAlso at Borough of Manhattan Community College, City University of New York, New York NY, United States of America
- ^eAlso at Center for High Energy Physics, Peking University, Beijing
- ^fAlso at Center for Interdisciplinary Research and Innovation (CIRI-AUTH), Thessaloniki, Greece
- ^gAlso at Centro Studi e Ricerche Enrico Fermi, Italy
- ^hAlso at CERN Tier-0, Switzerland
- ⁱAlso at CERN, Geneva, Switzerland
- ^jAlso at Département de Physique Nucléaire et Corpusculaire, Université de Genève, Genève, Switzerland
- ^kAlso at Departament de Física de la Universitat Autònoma de Barcelona, Barcelona, Spain
- ^lAlso at Department of Financial and Management Engineering, University of the Aegean, Chios, Greece
- ^mAlso at Department of Physics and Astronomy, University of Sheffield, Sheffield, United Kingdom
- ⁿAlso at Department of Physics and Astronomy, University of Victoria, Victoria BC, Canada
- ^oAlso at Department of Physics, Ben Gurion University of the Negev, Beer Sheva, Israel
- ^pAlso at Department of Physics, California State University, Sacramento, United States of America
- ^qAlso at Department of Physics, King's College London, London, United Kingdom
- ^rAlso at Department of Physics, Oxford University, Oxford, United Kingdom
- ^sAlso at Department of Physics, Royal Holloway University of London, Egham, United Kingdom
- ^tAlso at Department of Physics, Stanford University, Stanford CA, United States of America

- ^uAlso at Department of Physics, University of Fribourg, Fribourg, Switzerland
- ^vAlso at Department of Physics, University of Massachusetts, Amherst MA, United States of America
- ^wAlso at Department of Physics, University of Thessaly, Greece
- ^xAlso at Department of Physics, Westmont College, Santa Barbara, United States of America
- ^yAlso at Deutsches Elektronen-Synchrotron DESY, Hamburg and Zeuthen, Germany
- ^zAlso at Fakultät Physik, Technische Universität Dortmund, Dortmund, Germany
- ^{aa}Also at Fakultät für Mathematik und Naturwissenschaften, Fachgruppe Physik, Bergische Universität Wuppertal, Wuppertal, Germany
- ^{ab}Also at Group of Particle Physics, University of Montreal, Montreal QC, Canada
- ^{ac}Also at Hellenic Open University, Patras, Greece
- ^{ad}Also at Institutio Catalana de Recerca i Estudis Avancats, ICREA, Barcelona, Spain
- ^{ae}Also at Institut für Experimentalphysik, Universität Hamburg, Hamburg, Germany
- ^{af}Also at Institut für Physik, Universität Mainz, Mainz, Germany
- ^{ag}Also at Institute for Nuclear Research and Nuclear Energy (INRNE) of the Bulgarian Academy of Sciences, Sofia, Bulgaria
- ^{ah}Also at Institute of Applied Physics, Mohammed VI Polytechnic University, Ben Guerir, Morocco
- ^{ai}Also at Institute of Particle Physics (IPP), Canada
- ^{aj}Also at Institute of Physics and Technology, Ulaanbaatar, Mongolia
- ^{ak}Also at Institute of Physics, Azerbaijan Academy of Sciences, Baku, Azerbaijan
- ^{al}Also at Institute of Theoretical Physics, Iliia State University, Tbilisi, Georgia
- ^{am}Also at IRFU, CEA, Université Paris-Saclay, Gif-sur-Yvette, France
- ^{an}Also at L2IT, Université de Toulouse, CNRS/IN2P3, UPS, Toulouse, France
- ^{ao}Also at Lawrence Livermore National Laboratory, Livermore, United States of America
- ^{ap}Also at National Institute of Physics, University of the Philippines Diliman (Philippines), Philippines
- ^{aq}Also at Ochanomizu University, Otsuka, Bunkyo-ku, Tokyo, Japan
- ^{ar}Also at School of Physics and Astronomy, University of Birmingham, Birmingham, United Kingdom
- ^{as}Also at School of Physics and Astronomy, University of Manchester, Manchester, United Kingdom
- ^{at}Also at SUPA - School of Physics and Astronomy, University of Glasgow, Glasgow, United Kingdom
- ^{au}Also at Technical University of Munich, Munich, Germany
- ^{av}Also at The Collaborative Innovation Center of Quantum Matter (CICQM), Beijing
- ^{aw}Also at TRIUMF, Vancouver BC, Canada
- ^{ax}Also at Università di Napoli Parthenope, Napoli, Italy
- ^{ay}Also at University of Chinese Academy of Sciences (UCAS), Beijing
- ^{az}Also at University of Colorado Boulder, Department of Physics, Colorado, United States of America
- ^{ba}Also at Washington College, Chestertown, MD, United States of America
- ^{bb}Also at Yeditepe University, Physics Department, Istanbul, Türkiye
- [†]Deceased